

# The “Calamine” of Southwest Sardinia: Geology, Mineralogy, and Stable Isotope Geochemistry of Supergene Zn Mineralization

MARIA BONI,<sup>†</sup>

*Dipartimento di Geofisica and Vulcanologia, Università di Napoli “Federico II,” Via Mezzocannone 8, 80134-Napoli, Italy*

H. ALBERT GILG,

*Fakultät Chemie, Technische Universität München, Lichtenbergstr. 4, 8574-Garching, Germany*

GASPARE AVERSA,\*

*Dipartimento di Geofisica and Vulcanologia, Università di Napoli “Federico II,” Via Mezzocannone 8, 80134-Napoli, Italy*

AND GIUSEPPINA BALASSONE

*Dipartimento di Scienze della Terra, Università di Napoli “Federico II,” Via Mezzocannone 8, 80134-Napoli, Italy*

## Abstract

The mining district of southwest Sardinia, Italy, is one of the classic areas where primary carbonate-hosted Zn-Pb sulfide ores are associated with a relatively thick secondary oxidation zone containing Zn (hydroxy-)carbonates and silicates, the so-called “calamine,” exploited until the 1970s. The extent of the capping oxidized ore zones, reaching deep below the surface, is generally independent of the present-day water table. The base of the oxidation profile containing nonsulfide Zn minerals in various uplifted blocks in the Iglesias area can be both elevated above or submerged below the recent water table. The genesis of the ores is therefore considered to be related to fossil, locally reactivated, oxidation phenomena. The mineralogy of the nonsulfide mineralization is generally complex and consists of smithsonite, hydrozincite, and hemimorphite as the main economic minerals, accompanied by iron and manganese oxy-hydroxides and residual clays.

This study places the secondary ores in the context of the tectonostratigraphic and climatic evolution of Sardinia and includes a petrographic and mineralogic study of the most abundant minerals, relating the mineralogy of secondary Zn and Pb carbonates to their stable C and O isotope geochemistry and constraining the origin of the oxidizing fluids and the temperature of mineralization. The  $\delta^{18}\text{O}_{\text{VSMOW}}$  values of smithsonite are homogeneous, regardless of crystal morphology, position, and mine location (avg.  $27.4 \pm 0.9\%$ ). This homogeneity points to a relatively uniform isotopic composition of the oxidation fluid and corresponding formation temperatures of 20° to 35°C. Considering the karstic environment of smithsonite formation in southwest Sardinia, this high temperature could be due to heat release during sulfide oxidation. The carbon isotope compositions of secondary Zn carbonates display considerable variations of more than 9 per mil ( $\delta^{13}\text{C}_{\text{VPDB}}$  from  $-0.6$  to  $-10.4\%$ ). This large range indicates participation of variable amounts of reduced organic and marine carbonate carbon during sulfide oxidation. The isotopic variation can be related to a variation in crystal morphologies of smithsonite, reflecting different environments of formation with respect to water table oscillations in karstic environments (upper to lower vadose to epiphreatic). The same range in  $\delta^{13}\text{C}$  isotope values is displayed by the calcite associated with Zn carbonates and by recent speleothems.

The most reliable time span for the deposition of bulk calamine ore in southwest Sardinia ranges from middle Eocene to Plio-Pleistocene, although further multiple reactivation of the weathering profiles, peaking within the warm interglacial periods of the Quaternary, cannot be excluded.

## Introduction

THE RECENT revival of commercial interest in nonsulfide zinc ores (Large, 2001; Hitzman et al., 2003), related to the development of solvent-extraction and electrowinning technology applied to their treatment, is renewing scientific research focused on “zinc oxide” deposits throughout the world (e.g., Angouran, Iran: Annels et al., 2003; Gilg et al., in press a; Beltana, Australia: Groves and Carman, 2003; Shaimerden, Kazakhstan: Boland et al., 2003; Skorpion, Namibia: Borg et al., 2003).

In the Iglesias area of southwest Sardinia, Italy, one of the oldest districts in the world mined for base metals, notable occurrences of secondary nonsulfide Zn  $\gg$  Pb ores

(“calamine”) were found at the end of the nineteenth century by the Belgian company Vieille Montagne and exploited in several mines. Historically, the so-called “calamine” ores, a mixture of supergene zinc (with minor Pb) carbonates, hydroxy carbonates, and silicates, capping the primary sulfide bodies (Boni et al., 1996), were the principal source of zinc from this district for more than 60 years. Their characteristics were described in several mine reports (e.g., Münch and Siebdrat, 1960) and their spatial distribution and mineralogy were investigated by several authors (Billows, 1941; Cavinato, 1952; Zuffardi, 1952). However, only limited data exist in the recent geologic literature about the Sardinian calamine deposits (Moore, 1972; Bonifazi and Massacci, 1987). In Boni et al. (in press) and Aversa et al. (2002), the theme of calamine and of its relationship with primary sulfide ores was briefly

<sup>†</sup>Corresponding author, e-mail: boni@unina.it

\*Present address: Department of Geology, Rand Afrikaans University, P.O. Box 524, Auckland Park 2006, South Africa.

discussed for the first time in the context of the geological and geomorphological evolution of Sardinia, with a detailed mineralogical study, as well.

The most important problems regarding this type of mineralization are (1) the tectonic, climatic, and hydrologic conditions that caused dissolution of the primary sulfides together with the host carbonate rocks, followed by the deposition of nonsulfide Zn deposits (2) the nature and provenance of the fluids associated with the calamine ores, and (3) the time constraints for the powerful oxidation phenomena that generated the calamine ores.

This study addresses these questions by placing the calamine ores in the context of the tectonostratigraphic and climatic evolution of this part of Sardinia, examining the relationship of the calamine with the primary ore types, conducting a thorough petrographic and mineralogical study of the

main economic oxidation minerals, and relating the mineralogy of secondary Zn and Pb carbonates, as well as recent Ca carbonates of meteoric origin, with their stable C and O isotope geochemistry, thus constraining the origin of the oxidizing fluids and the temperature of mineralization.

### Geologic Setting

The geology of southwest Sardinia is largely dominated by Paleozoic rocks of sedimentary as well as igneous origin (Fig. 1). Among the sedimentary successions, Cambro-Ordovician rock types predominate. These units are epizonal facies low-grade metamorphic rocks and belong to the so-called "external zones" of the Variscan orogen (Carmignani et al., 1994).

The Lower Cambrian succession is subdivided into the basal Nebida Group, which consists of 400 to 500 m of siliclastic sedimentary rocks, with carbonate intercalations toward

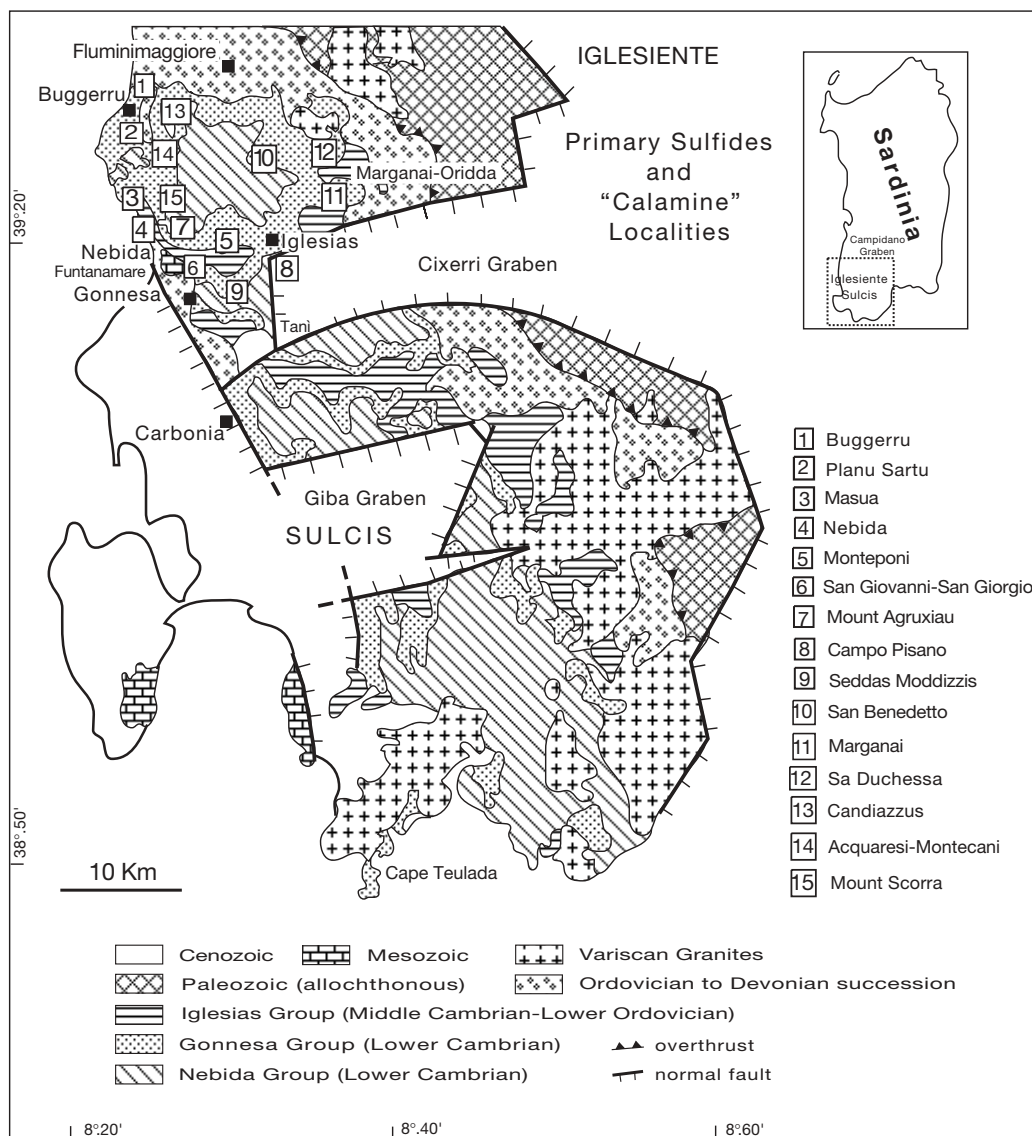


FIG. 1. Geologic sketch map of southwest Sardinia with location of the "Calamine" orebodies; the calamine at Candiazus, San Benedetto, Seddas Moddizzis, and Campo Pisano are derived from sedex sulfides, whereas in Buggerru, Planu Sartu, Masua, Monteponi, San Giovanni, Mount Agruxiau, Marganai, Sa Duchessa, Mount Scorra, Montecani, Acquaresi, and San Giorgio the primary ores were Mississippi Valley-type (modified from Bechstadt and Boni, 1994).

the top, and the overlying Gonnesa Group, which consists of 300 to 600 m of shallow-water platform carbonate rocks (Bechstadt and Boni, 1994). Strata-bound sulfides and barite deposits are hosted by Lower Cambrian sedimentary rocks. Middle and Upper Cambrian-Lower Ordovician strata are represented by nodular limestones (Campo Pisano Formation, Iglesias Group, 50–80 m) and slates (Cabitza Formation, Iglesias Group, 400 m) respectively. The Cambrian to Lower Ordovician sedimentary rocks were extensively deformed during the intra-Ordovician “Sardic” tectonic phase. Erosion and deposition of Upper Ordovician, as well as Silurian, sedimentary rocks followed on an angular unconformity over the Cambrian deposits.

At least two compressional phases of deformation with penetrative schistosity are related to the Devonian-Carboniferous Variscan orogeny (Carmignani et al., 1994), which resulted in vertical tilting of the whole lower Paleozoic succession. The Paleozoic basement was later affected by several types of magmatic intrusions in a time span from Late Carboniferous to Permian. A strong pervasive hydrothermal dolomitization (“Geodic dolomite”: Boni et al., 2000) of possible Permian age affected large volumes of the Cambrian limestones in the area.

The late Variscan uplifts were followed by several pulses of extensional tectonics causing repeated opening of fractures during the Mesozoic as well as circulation of hydrothermal fluids (Boni et al., 1992; 2001). A widespread erosion peneplane developed in the Iglesias-Sulcis region at this time. This event was followed by deep karstification in the Cambrian carbonate rocks. The karstic network was almost completely filled by internal carbonate sediments (calcite and dolomite), collapse breccias, and hydrothermal cements. These rocks were locally subjected to late hydrothermal silicification. Rare marine sedimentary rocks of Mesozoic age are restricted to the western margins of the peneplaned massif. By the end of the Mesozoic, Sardinia was completely emerged.

Tertiary sedimentary and volcanic rocks are fairly widespread throughout the whole region. Among the former are the marly calcareous sedimentary rocks (“Miliolitico”) of the Sulcis basin (early to middle Eocene) that contain brown coal deposits. These coals were deposited in a graben area resulting from extensional tectonic events at the southeastern edge of the Iberian plate (Assorgia et al., 1992), then unconformably covered by red arenaceous continental sedimentary rocks of the (middle to late Eocene?) Cixerri Formation (Cherchi and Montadert, 1982). The Pyrenaic phase of the Alpine orogeny was responsible for this unconformity. The Cixerri Formation is of utmost importance in southwest Sardinia because it represents the last continental sedimentation on the emerged continent before the opening of the western Mediterranean basin (Carmignani et al., 1989). In many areas of the Sulcis region, at the base of the Cixerri Formation a thick lateritic horizon caps the Paleozoic as well as Eocene(?) carbonate rocks. The laterite contains red clays and iron-rich oolitic concretions as well as detrital fragments of pre-Tertiary barite (Salvadori, 1961).

A strong karstic dissolution in the calcareous basement, although not very deep, could have accompanied the pre-Cixerri emersion and lateritization phases. The development of

the microkarstic and macrokarstic network in the Cambrian limestones was clearly promoted by the aggressive character of the circulating waters and the high sulfide content of the carbonate rocks undergoing dissolution.

Following deposition of the Cixerri Formation, another phase of widespread tensional tectonics of middle Oligocene age produced a large rift system mostly in the western part of Sardinia (Campidano, Cixerri, Giba grabens). This rifting was accompanied by the deposition of synrift, continental sedimentary rocks, thus emphasizing the role of the faults. An important episode of Oligocene-Miocene andesitic to rhyolitic and rhyodacitic volcanism was initiated by the counterclockwise rotation of the Corsica-Sardinia microplate. This episode is also evident in the southwest of the island, marking the lineaments controlling the east-west oriented tectonic graben of Cixerri in Iglesias and Giba in Sulcis.

During the Miocene and Pliocene, Sardinia was subjected to several emersion-erosion phases, alternating with marine transgressions and volcanic episodes of calc-alkaline to alkaline basalts. A strong Plio-Pleistocene tensional tectonic phase was responsible for the final deepening of the Campidano graben and, most probably, the differentiated uplift of the Paleozoic basement. In fact, faulting during the last phases of the Alpine orogeny ruptured the Paleozoic massifs into a series of stepped fault blocks in both the Iglesias and Sulcis areas.

Pleistocene deposits in southwest Sardinia consist of rare marine sedimentary rocks along the coasts as well as eolian dunes and karstic cavity fillings of both chemical (speleothem concretions) and detrital (collapse breccias and terra rossa) nature. The latter commonly include fossil remnants of terrestrial organisms (such as mammals), all recording the Tyrrhenian warm interglacial stages. Conglomerates of fluvial origin and Holocene sand dunes characterize the coastal belt northwest of Gonnesa, whereas small travertine deposits (Tani, Funtanamare; Fig. 1) occur along the flanks of the Cambrian carbonate rocks.

When investigating the timing of the nonsulfide deposits in a given area, one must consider the ages of the various stages of tectonic uplift and peneplanation of utmost importance. It is also necessary to relate them to climatic oscillations recorded both at a global and local scale to document the major constraints on the oxidation and preservation of the deposits. What makes this task difficult in southwest Sardinia is the lack of precise geologic constraints on the development of the (probably numerous) karstification phases that are closely related to formation of the calamine ores.

## Ore Deposits

### *Primary sulfide deposits*

The largest Zn-Pb-Ba Sardic mines were in Iglesias (Fig. 1). Most of the exploited orebodies are pre-Variscan in age. Some post-Variscan deposits (in the form of vein and paleokarst filling) were economic in the past (Boni, 1985; Bechstadt and Boni, 1994; Boni et al., 1996; Boni et al., 2001). The pre-Variscan orebodies are stratiform and/or strata bound and are hosted in the Lower Cambrian carbonate rocks (Gonnesa Group). They are the result of a combination of favorable sedimentary

environments and Paleozoic tensional tectonics. Two groups of genetically distinct ore types are known: (1) syngenetic-early diagenetic massive sulfides (pyrite >> sphalerite >> galena) in the tidal dolomites of the lower Gonnesa Group (Santa Barbara Formation), interpreted as sedimentary exhalative (sedex) deposits, and (2) void-filling, breccia cement, and late-diagenetic replacement bodies (sphalerite > galena >> pyrite) in the shallow water limestones of the upper Gonnesa Group (San Giovanni Formation), interpreted as Mississippi Valley-type deposits (Boni et al., 1996).

The pre-Variscan mineral deposits have been deformed and sheared by Variscan compressional tectonics. The strata-bound ores have been strongly tilted with their host carbonate rocks, commonly to a vertical attitude, thus rendering easier the recharge and circulation of meteoric waters responsible for dissolution and secondary oxidation.

At the end of Variscan compression, local intrusions of calcalkaline granitoids at shallow depths caused the formation of calcic skarns of the Zn-Pb(-Cu) type. This mineralization rarely reached economic grade, and then only where the concentrations were controlled by stratigraphic contacts between different rock types and in fault zones.

Between the end of the Variscan orogeny and the beginning of the Alpine cycle, southwest Sardinia was the site of several widespread mineralization events comparable to those that occurred in other parts of central and western Europe (Boni et al., 1992; Boni et al., 2001). These events resulted in widespread hydrothermal dolomitization ("Dolomia Geodica") of the lower Paleozoic carbonate rocks (Boni et al., 2000) and in a variety of base metal-Ba-F vein and paleokarst deposits associated with distinctive low-temperature and high-salinity fluids. They are characterized by a simple mineral association consisting of Ag-rich galena and barite. Deposit tonnages are quite low but, owing to their high Ag content, they were originally exploited by the Phoenicians and Romans and then in the Middle Ages by the Pisans.

Further hydrothermal activity of unknown age (Tertiary?), not related to any metal deposition, is thought to have been responsible for the precipitation of widespread scalenohedral calcites (De Vivo et al., 1987) that coat the deep phreatic conduits of the Cambrian limestone. The hydrothermal fluids were less saline than the Permo-Mesozoic mineralizing fluids.

### *Secondary nonsulfide deposits*

The nonsulfide zinc deposits in the Iglesias district belong to the carbonate-hosted "calamine" category (Large, 2001), in which smithsonite, hydrozincite, and hemimorphite are the principal zinc-bearing minerals. Cerussite and angle-site also occur, generally associated with nodules and lenses of residual or supergene galena. A complex association of iron and manganese oxy-hydroxides, with a characteristic red-brown staining (goethite, lepidocrocite, hematite), and residual clay minerals hosts the nonsulfide ore. The mineralogy of the ores is generally complex and comprises not only the most common Zn and Pb carbonates and silicates but also exotic species (Billows, 1941; Moore, 1972; Stara et al., 1996). The ore grade of the "calamine" is recorded to have been highly variable throughout the mining district, ranging from a few percent of combined Zn-Pb to more than 30 percent in the areas where the alteration profile resulted in a complete

replacement of the sulfides by secondary carbonates. Both calcite and aragonite are common accessory minerals in many Sardinian Zn-Pb "calamine" ores.

The calamine ores are particularly enriched in Zn in the lower levels of the oxidation profile, whereas near the surface (in the leaching zone) the ore grades were generally not economic. In the upper levels of the mines, secondary silicate phases predominate and strong silica replacement of the carbonates occurs locally (Zuffardi, 1952; Münch and Siebdrat, 1960). The Zn carbonate ore shoots in most Iglesias mines are roughly located within the lower vadose zone of a karstic system that is hundreds of meters deep but above the water-filled conduits of the phreatic saturated zone, where the deposition of secondary supergene sulfides (galena and Cu sulfides) is known to occur locally.

The mineralization is considered to be the result of the in situ oxidation of the primary sulfide ores by meteoric fluids, with increased acidity owing to the dissolution of substantial amounts of pyrite, that circulated through the carbonates (Cavinato, 1952; Zuffardi, 1952; Moore, 1972). The dissolution was followed by a more or less complete replacement of the sulfide phases, as well as of parts of the host rocks, by secondary minerals. A distinct oscillatory zoning (zinc-enriched and zinc-poor bands: Zuffardi, 1952) in the deposits of the Iglesias Valley is considered to have been caused by fluctuations in the water table, cyclically altering the regular deepening grade of the oxidation profiles. A subsequent remobilization and redeposition within dissolution vugs and karst cavities of the newly formed oxidation minerals locally followed the replacement process.

Several styles of "calamine" have been recognized throughout the district, including both partial replacement of the host carbonates and strata-bound primary sulfides (so-called "calamine roche" by the old miners), as well as concentrations of detrital, ferruginous, "earthy" smithsonite and hemimorphite-rich clays ("calamine terre"). The latter generally fill a maze of interconnecting (meters to tens of meters long) karst cavities and open conduits in the upper levels of the mines.

There is a marked difference between the form and the general metal content of the main nonsulfide ores, depending on whether they were derived from the massive sulfides (sedex) or from the Mississippi Valley-type ores hosted in the Cambrian limestone (Zuffardi, 1952). In the first case (San Benedetto, Campo Pisano, and Seddas Moddizis mines), despite the abundance of iron oxides and the difficulty of the exploitation owing to the instability of mine workings, the ore grade was always higher, the oxidation process complete, and the beneficiation easier. The calamine ores that originated from massive sulfides completely replaced the primary orebodies, without apparent reaction with the dolomite host rocks. These ores generally belong to the earthy "calamine terre" type and are not constrained by a rigid limestone framework. They do not contain galena or cerussite, because PbS was absent in the primary massive sulfides ore. In the case of calamine derived from Mississippi Valley-type ore in the limestone, smithsonite and hemimorphite were always accompanied by galena, and even by sphalerite, and the ore grade was generally lower. These ores are of the "calamine roche" type. In these ores the oxidation was quite irregular, and the formation of the economic deposit was constrained

not only by the form of the primary sulfides but also by the extension and depth of the karstic network.

From mining records and the geologic evidence in the old open pits, it can be deduced that the calamine deposits in the whole Iglesias district extend downward between 200 and 500 m below the surface of the post-Variscan erosion peneplane (Zuffardi, 1952; Moore, 1972; Fig. 2). Partial oxidation can extend a further 100 m before completely unaltered sulfide ores are encountered at depth. The base of the oxidation profile is seldom coincident with the present water table (except in Buggerru area), but it is elevated above it (Marganai-Orida district in the east) or submerged beneath it (Iglesias Valley, Nebida coastal belt) within different blocks that are delimited by (possibly) Tertiary faults (Moore, 1972). The measured thickness of the oxidation zone visible today can exceed 600 m, reaching below current sea level in some areas. An old drill hole to the bottom of the Iglesias Valley (100 m a.s.l.), encountered oxidation minerals at a depth of 850 m b.s.l. (Marcello et al., 1965), suggesting that the whole thickness of the oxidation zone was even greater. These differences in the levels of the oxidation zone reflect several distinct episodes of Tertiary and possibly Plio-Quaternary block faulting, which displaced to different elevations the mature, though still evolving, oxidation profiles developed in the Cambrian carbonate rocks.

*Buggerru (northwestern Iglesias):* The calamine at the Buggerru-Planu Sartu mining sites (Fig. 1) reach the present water table and merge with sulfide deposits a few tens of meters a.s.l., thus constraining the time of alteration of the primary ores. However, the deepest levels (50 m b.s.l.) reached by the old workings at Buggerru, still carried exploitable calamine (Zuffardi, 1952). The oxidized ores, mostly consisting of smithsonite, occurred along almost concordant layers of the Lower Cambrian limestone or as an earthy-looking matrix of dissolution breccias. Moderate silicification in the uppermost horizons of the deposit coincided with lower ore grades and the occurrence of transported "calamine terre."

*Iglesias and Nebida (western and southern Iglesias):* In the mines (Fig. 1) exploited in the carbonate blocks along the coast (Nebida-Masua; Fig. 3a) or in the hills bordering the Iglesias Valley (Monteponi, San Giovanni, Seddas Moddizis, Monte Agruxiau, Campo Pisano), oxidation extends 100 to 150 m below the present water table. In the Monteponi, Campo Pisano, and Masua mines, a zone of partial alteration, wherein newly formed calamine coexisted with residual or supergene sulfides (the "semiossidati" ore zone of the old miners; Fig. 3b), has been recorded well below the current sea level. This consistent submergence of the oxidation profiles is considered to be the result of downward movements of the whole block after the generalized post-Variscan peneplanation, the tensional tectonics active throughout the Mesozoic, and the generalized uplift that followed the Eocene marine ingression in the Sulcis basin.

A stepwise reactivation of the alteration profile, with local replacement of earlier-deposited supergene mineral phases by others adapted to new hydrologic conditions (i.e., smithsonite replaced by hydrozincite and/or hemimorphite), has been recorded in this part of the Iglesias. This reactivation could be due to either the renewed Plio-Pleistocene tensional tectonics or lowering of sea level owing to the modification of

climatic conditions at a global scale (e.g., Messinian evaporation in the Mediterranean realm or Quaternary glacial periods).

This rejuvenation created allochthonous false "gossans" on the surface and detrital deposits of transported calamine ("calamine terre") in a network of newly formed karstic cavities and open fractures largely above the current water table. A further karstic dissolution of the Cambrian carbonate rocks also occurred along newly generated fractures (or enlargement of the old conduits), followed by the deposition of both colloidal concretions (Fig. 3c) and stalactitic speleothems of Cd-rich smithsonite (Fig. 3d, e). These phenomena occurred throughout the district, but mostly in the Iglesias Valley and along the Nebida coastal belt. Another interesting phenomenon related to the lowering of the water table in the area is the local outcropping of fragments of phreatic caves filled by scalenohedral calcites crystals that were first coated by smithsonite and hemimorphite and then leached in their internal part, creating void casts.

*Marganai (southeastern Iglesias):* In the uplifted areas of northeastern Marganai and Orida (Fig. 1), the latter bordering the Variscan granite intrusions, the oxidation profiles are less developed and the ore restricted to the base of the now suspended fault-controlled Tertiary valleys (Moore, 1972). The better-known orebodies were exploited in the Sa Duchessa and Barrasciutta mines, where interesting enrichment horizons with secondary sulfides were also known. At the Sa Duchessa mine, where the primary sulfides (chalcopryrite and sphalerite) were associated with garnetiferous skarn emplaced at the contact with the Tiny granite, the main minerals exploited in the oxidation zone consisted of chrysocolla and malachite, with minor amounts of Cu-hemimorphite. At Barrasciutta, Zn-Cu calamine were exploited from several ill-defined allochthonous bodies in a maze of deep paleokarstic cavities. Textural studies of the ore minerals (Moore, 1972) showed that in the copper-rich Marganai zone, the secondary sulfides (chalcocite, bornite, and covellite) are themselves undergoing alteration. This alteration suggests that the earlier oxidation profile was related to a water table higher than the present one and that recent erosion has reached the supergene sulfide zone.

## Sampling and Analytical Methods

### Sampling

Notwithstanding the depth of the oxidation zone, a thorough sampling of the calamine was possible in a few still-accessible underground mining sites. Other specimens were sampled in mine dumps and from private collections. Up to 35 samples were collected of each ore type. Stable isotope analyses were carried out mainly on smithsonite and a few samples of hydrozincite, cerussite, and phosgenite (Table 1).

A number of Quaternary freshwater carbonates, calcite cements from Pleistocene bone beds, and Holocene travertines were also sampled. Ca carbonate crystals and concretions, paragenetically associated with calamine in several mines, were sampled to compare their stable isotope geochemistry with that of Zn carbonates, together with samples of internal sedimentary rocks from palaeokarstic hydrothermal deposits (Boni et al., 1992), scalenohedra of hydrothermal calcite (Masua mine, De Vivo et al., 1987), and carbonate soils

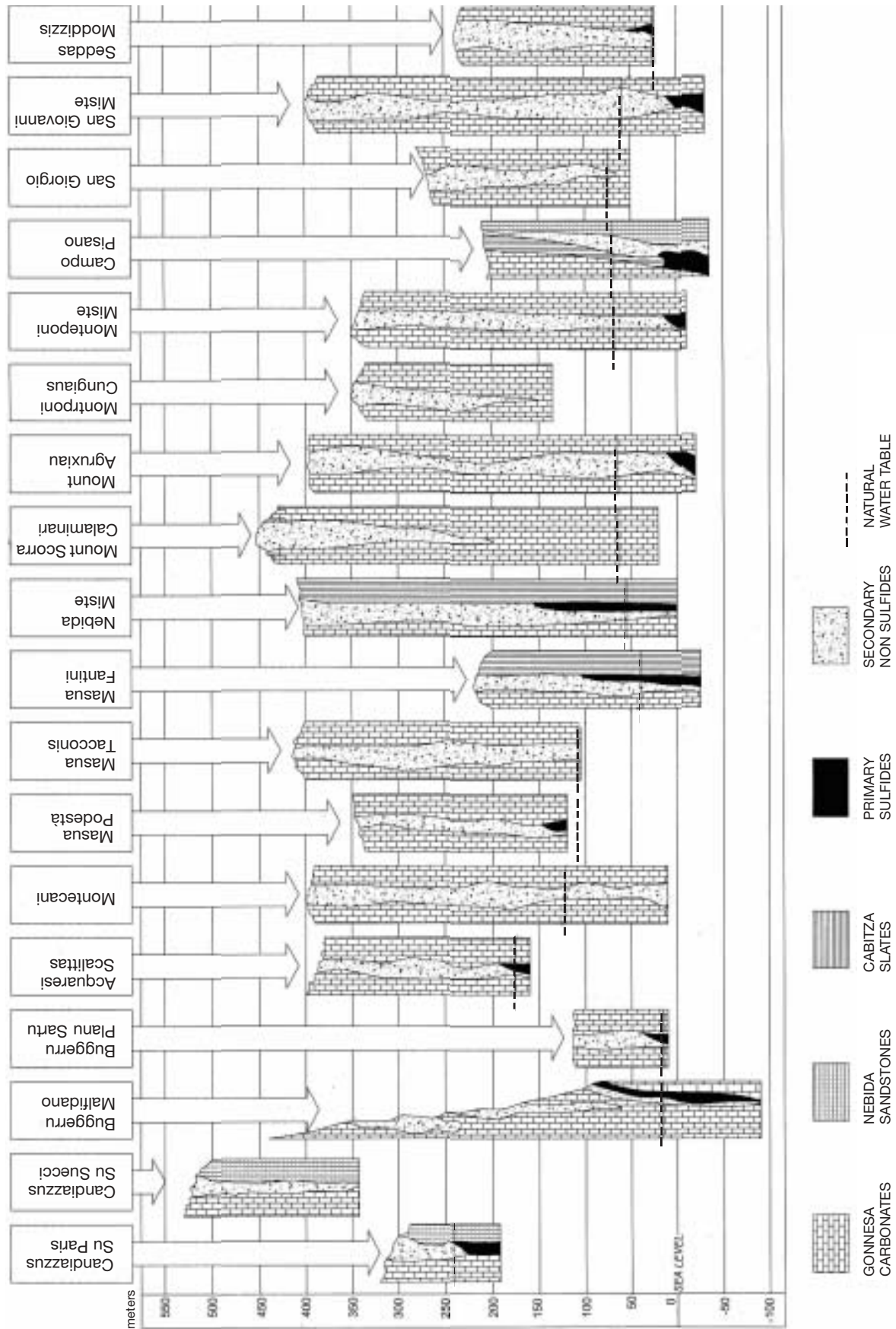


FIG. 2. Schematic representation of the depth of the oxidation level in various mines of the Iglesias district compared with the depth of the present water table (modified from Zuffardi, 1952). Note that in most cases primary bedding dips vertically.

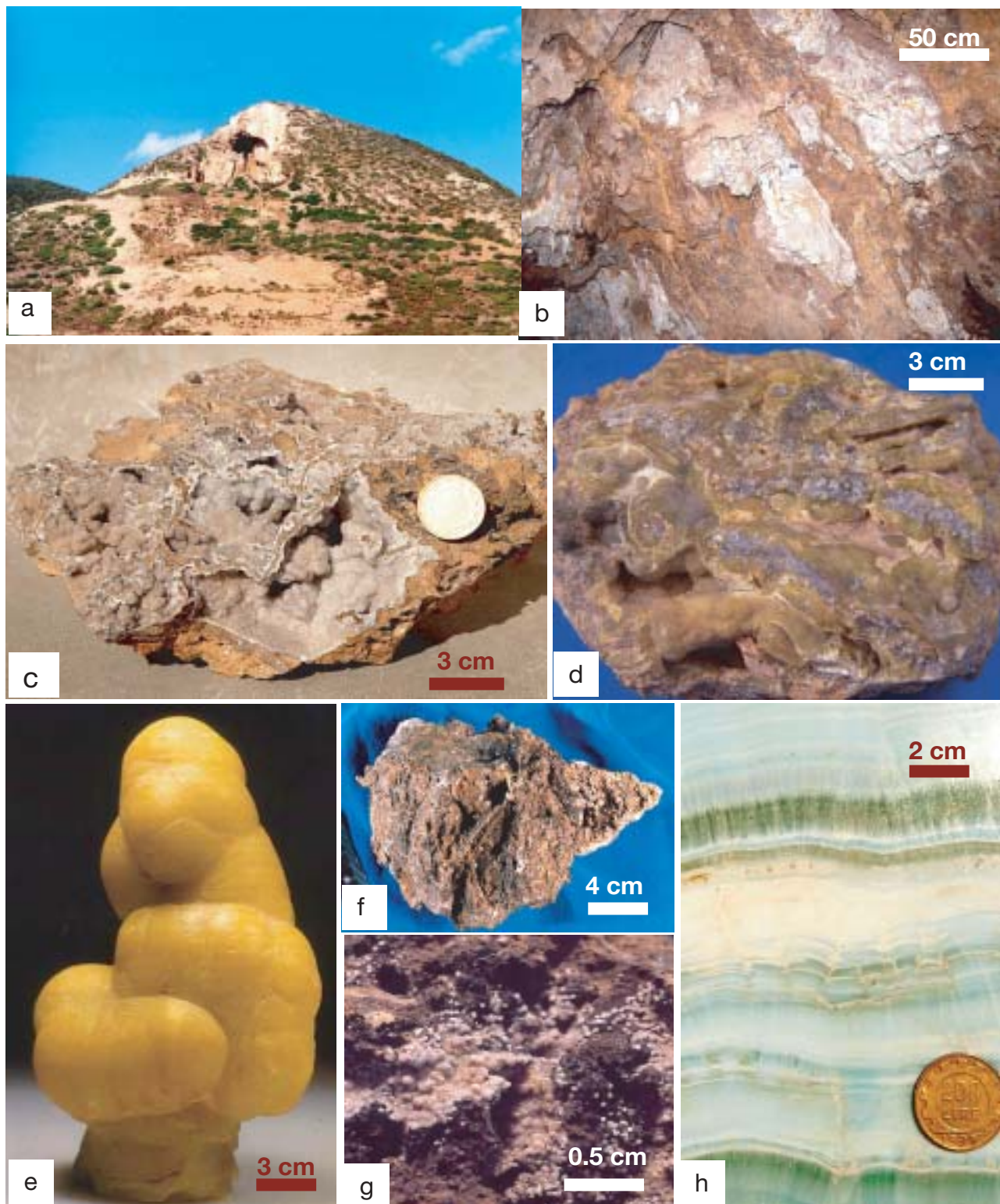


FIG. 3 a. Nebida-Massa Carroccia: old Calamine ore exploitation, started in open pit and deepened underground. b. Nebida-Santa Margherita, +92 level: "semiossidati" ores. c. Monteponi: Calamine concretionary crust on hydrothermal "gedic" dolomite; coin is 2.5 cm. d. Masua: Cd-rich concretionary smithsonite (Museo di Mineralogia, University of Napoli). e. Masua-Montecani: Cd-rich, stalactitic smithsonite (collection Manunta). f. Nebida-Santa Margherita +92 level: "Calamine roche." g. Mount Agruxiau: small globular smithsonite aggregates on dolomite. h. San Giovanni mine: green aragonite speleothem; coin is 2.5 cm.

TABLE 1. Carbon and Oxygen Isotope Data of Zn, Pb, and Ca ( $\pm$  Mg) Carbonates from Southwest Sardinia

Sample	Mineral (type)	Description	Location	$\delta^{13}\text{C}_{\text{VPDB}}$ (‰)	$\delta^{18}\text{O}_{\text{VSMOW}}$ (‰)
12-G	sm (I)	Clear rhombohedral crystals	<b>M</b> Nebida level +92	-10.44 <sup>1</sup> , -10.30 <sup>1</sup>	26.04, <sup>1</sup> 26.09 <sup>1</sup>
13-G	sm (I)	Dark rhombohedral crystals	<b>M</b> Nebida level +92	-10.15 <sup>1</sup> , -10.01 <sup>1</sup> , -10.49	27.05, <sup>1</sup> 27.44, <sup>1</sup> 27.61
13-Ga	sm (I)	Massive smithsonite	<b>M</b> Nebida level +92	-9.32	28.79
20-Ga	sm (I)	Massive smithsonite	<b>M</b> Seddas Moddizzis	-5.70	26.15
25-Ga	sm (I)	Massive smithsonite	Nebida Can.San Giuseppe	-4.90	27.29
29-Ga	sm (I)	Massive smithsonite	<b>M</b> Mount Agruxiau	-3.95	28.52
48-Ga	sm (I)	Massive smithsonite	<b>M</b> Nebida level +92	-8.75	27.96
49-G	sm (I)	Massive smithsonite	<b>M</b> Nebida level +92	-7.74	28.79
50-G	sm (I)	Clayey massive smithsonite	<b>M</b> Nebida level +92	-7.32	28.72
65-G	sm (I)	Pseudomorph after calcite	<b>M</b> Campo Pisano	-6.16	28.84
27-G	sm (II)	Rounded leached crystals	<b>M</b> Seddas Moddizzis	-6.80 <sup>1</sup>	27.54 <sup>1</sup>
Sar1a	sm (II)	White powdery coating Sar1	<b>M</b> Masua-Lanusei	-7.08	27.48
Sar1b	sm (II)	Orange crust coating Sar1	<b>M</b> Masua-Lanusei	-7.90	28.85
8-G	sm (III)	Yellow "rice grain" crystals	<b>M</b> Mount Agruxiau	-6.38 <sup>1</sup> , -6.37 <sup>1</sup> , -6.49	28.03, <sup>1</sup> 27.62, <sup>1</sup> 28.44
9-G	sm (III)	White "rice grain" crystals	<b>M</b> Mount Agruxiau	-6.90 <sup>1</sup>	28.00 <sup>1</sup>
18-G	sm (IV)	Crust (platy crystals)	<b>M</b> San Giovanni	-8.17 <sup>1</sup> , -8.21 <sup>1</sup> , -8.31	27.37, <sup>1</sup> 27.39, <sup>1</sup> 27.53
36-G	sm (IV)	Concretion (platy crystals)	<b>M</b> San Benedetto	-7.95 <sup>1</sup>	27.90 <sup>1</sup>
63-G	sm (IV)	Concretion (platy crystals)	<b>M</b> Monteponi-Cungiaus	-5.83	27.41
Sar1	sm (V)	Yellow Cd-stalactite	<b>M</b> Masua-Lanusei	-2.42 <sup>1</sup> , -2.40 <sup>1</sup>	26.70, <sup>1</sup> 26.82 <sup>1</sup>
Sar2b	sm (V)	Gray concretion	<b>M</b> Monteponi	-3.17	28.51
20-G	sm (V)	Rose concretion	<b>M</b> Seddas Moddizzis	-3.78 <sup>1</sup> , -3.95	25.51, <sup>1</sup> 25.85
25-G	sm (V)	Yellow concretion	Nebida Can.San Giuseppe	-1.99 <sup>1</sup> , -2.03	26.36, <sup>1</sup> 26.72
24-G	sm (V)	Botryoidal concretion	Nebida Can.San Giuseppe	-1.78 <sup>1</sup> , -1.78 <sup>1</sup>	26.52, <sup>1</sup> 26.44 <sup>1</sup>
52-G	sm (V)	White stalactite	<b>M</b> San Giovanni	-2.01	28.04
64-G	sm (V)	Small white concretion	<b>M</b> Monteponi-Cungiaus	-0.59	27.48
5-G	Fe-sm	"Monheimite" crystals	<b>M</b> Montevecchio	-5.14 <sup>1</sup> , -4.82	20.39, <sup>1</sup> 21.01
Sar-3	hz	White powder	<b>M</b> San Giovanni	-7.06 <sup>1</sup>	27.04 <sup>1</sup>
45-G	hz	Botryoidal crust	<b>M</b> Monteponi	-2.61 <sup>1</sup> , -2.24	26.53, <sup>1</sup> 26.67
10-G	ce	Crystals	<b>M</b> Monteponi	-11.63	17.12
11-G	ce+hz	Hz encrustation on 10-G	<b>M</b> Monteponi	-11.22 <sup>1</sup>	19.48 <sup>1</sup>
MP-1	pg	Clear crystals	<b>M</b> Monteponi	-7.16	21.06
MP-3	pg	Clear crystals	<b>M</b> Monteponi	-9.24	20.67
56-G	do	Hydrothermal dolomite	Buggerru	-0.73	21.79
60-G	do	Hydrothermal dolomite	Buggerru	-3.73	23.67
43-G	cc	Scalenohedral crystal	<b>M</b> Masua	-3.45 <sup>1</sup>	15.12 <sup>1</sup>
55-Ga	cc	Intern. sediment in paleokarst	<b>M</b> San Giovanni	-1.08	18.03
55-G	cc	Crystals on 55-Ga	<b>M</b> San Giovanni	-2.87	20.36
46-G	cc	Triassic caliche	Nebida	-7.02 <sup>1</sup>	25.82 <sup>1</sup>
1-G	cc	Holocene travertine	Tani	-9.58 <sup>1</sup>	25.75 <sup>1</sup>
3-G	cc	Holocene travertine	Funtanamare	-8.74 <sup>1</sup>	25.57 <sup>1</sup>
4-G	ar	Subrecent stalactite	<b>M</b> Monteponi	-0.61 <sup>1</sup>	26.16 <sup>1</sup>
7-G	ar	Lower vadose speleothem	Seddas De Daga (Iglesias)	-7.09 <sup>1</sup> , -7.15 <sup>1</sup>	25.51, <sup>1</sup> 26.56 <sup>1</sup>
44-G	ar	Green speleothem	<b>M</b> San Giovanni	-5.60 <sup>1</sup>	26.25 <sup>1</sup>
21-G	cc	Subrecent stalactite	Grotta San Giovanni	-2.55 <sup>1</sup>	29.05 <sup>1</sup>
66-G	cc	Concretion in red bone bed	Nebida	-1.30	27.54
33-G	cc	Concretion with calamine	<b>M</b> Nebida-Carroccia	-9.21 <sup>1</sup>	24.66 <sup>1</sup>
38-G	cc	Crystals with calamine	<b>M</b> Monteponi-Nicolay	-9.76 <sup>1</sup>	25.57 <sup>1</sup>
40-G	cc	Crystals with calamine	<b>M</b> Monteponi-Villamarina	-10.09 <sup>1</sup>	24.81 <sup>1</sup>
41-G	cc	Crystals with calamine	<b>M</b> Monteponi-Villamarina	-10.17 <sup>1</sup>	24.81 <sup>1</sup>
62-G	cc	Crystals with calamine	<b>M</b> Buggerru	-11.28	25.39

Abbreviations: ar = aragonite, cc = calcite, ce = cerussite, do = dolomite, hz = hydrozincite, **M** = mine, ph = phosgenite, sm = smithsonite (see text for descriptions of types I to V)

<sup>1</sup> Conventional analyses (dual inlet MS), all other unmarked analyses using continuous flow technique

(“caliche”) occurring at the base of the Triassic Campumari Formation (Nebida). The main goal of this additional sampling was to determine whether other rock types besides the host Cambrian dolostones and limestones (Boni et al., 1988) could have contributed to the isotopic signature of the carbon in the fluids that precipitated the Zn carbonates.

#### Analytical methods

Each mineral phase was enriched by combined magnetic and gravimetric separation techniques, then examined under the stereomicroscope and polarizing microscope. Particular care was undertaken in selecting the Zn carbonate specimens for isotopic analyses.

Mineral identification by X-ray powder diffraction analysis (XRPD) was carried out with an automated diffractometer (Seifert MZVI) with  $\text{CuK}\alpha$  radiation (1.5406 Å, 40 kV, 30 mA) between  $5^\circ$  and  $75^\circ(2\alpha)$  and  $0.5^\circ 2\alpha/\text{min}$ . Synthetic  $\text{CaCO}_3$  was used as an internal standard. The position of the 1014 reflection for  $\text{CaCO}_3$  was taken as 3.035 Å, JCPDS-ICDD (Joint Committee on Powder Diffraction Standards-International Centre for Diffraction Data)-5-586. The program XDATA was used to evaluate the analyzed spectra. Diffraction patterns were compared with both the JCPDS-ICDD database and other literature data. Least-squares refinement of 20 reflections was used for accurate unit-cell determination.

Scanning electron microscope (SEM) observations and major element analyses were performed on a Jeol JSM-5310, in energy-dispersive mode spectrometer (EDS) (Link Analytical 10000), and semiquantitative compositions were reduced by a ZAF correction program. Silicates, oxides and pure elements were used as standards. Operating conditions were 15 kV acceleration voltage and  $10 \mu\text{m}$  spot size. The water content was evaluated by means of thermal analyses.

Stable oxygen and carbon isotope ratios were determined on  $\text{CO}_2$  released from carbonate minerals by reaction with anhydrous phosphoric acid using two different techniques. The first technique, performed in the Stable Isotope Laboratory at Technische Universität München, Germany, follows the standard sealed vessel method of McCrea (1950). This procedure uses a temperature-controlled water bath and reaction temperature of  $25^\circ\text{C}$  with reaction times of circa 15 h for highly reactive minerals, such as calcite, aragonite, cerussite, phosgenite, and hydrozincite, and a higher reaction temperature ( $50^\circ\text{C}$ ) and longer reaction time (three days) for the more refractory minerals smithsonite, Fe smithsonite (“monheimite”), and dolomite. The evolved  $\text{CO}_2$  gas was purified and analyzed on a Finnigan MAT251 dual-inlet isotopic ratio mass spectrometer.

The second technique, performed at the Bayerische Staatssammlung für Paläontologie, Munich, Germany, employed an automated on-line device operated in the continuous-flow mode (Finnigan Gasbench II). Individual reaction tubes were heated to  $72^\circ\text{C}$  at reaction times of 1.5 h in combination with a Finnigan Deltaplus mass spectrometer.

On the basis of repeated measurements of laboratory and international standards (NBS-18, NBS-19), the precision of the isotopic analyses is better than 0.1 per mil ( $1\sigma$ ) for both techniques. Oxygen isotope analyses were corrected using the phosphoric acid fractionation factors for calcite and aragonite

(1.01024 at  $25^\circ\text{C}$ : Swart et al., 1991), cerussite (1.01061 at  $25^\circ\text{C}$  and 1.00911 at  $72^\circ\text{C}$ : Gilg et al., in press), smithsonite (1.01052 at  $50^\circ\text{C}$  and 1.00958 at  $72^\circ\text{C}$ : Gilg et al., in press), and dolomite (1.00986 at  $72^\circ\text{C}$ : Rosenbaum and Sheppard, 1986). Phosphoric acid fractionation factors are not known for hydrozincite and phosgenite. As these minerals react rapidly with the acid at  $25^\circ\text{C}$ , the phosphoric acid fractionation factors of calcite were used for these minerals (O’Neil, 1986; Melchiorre et al., 1999, 2000; Gilg et al., in press b).

#### Mineralogy

The principal nonsulfide zinc minerals of economic significance recognized in the mining district are smithsonite, hydrozincite, and hemimorphite. Cerussite also occurs in the mineral assemblage of the samples from Nebida and Monteponi mines. Anglesite and phosgenite have been observed locally in the Monteponi mine (Moore, 1972). Among gangue minerals, calcite is quite ubiquitous (no newly precipitated dolomite, ankerite, or siderite has been detected), followed by minor quartz, iron oxy-hydroxides, and residual barite. A detailed report of the mineralogy has been presented elsewhere (Aversa et al., 2002). The main assemblages are described below.

#### Smithsonite and hydrozincite

Smithsonite is widespread and occurs in different types of aggregates ranging in color from grayish white, light yellow, or pink to a dark gray. An extensive SEM study carried out on a large number of smithsonite-bearing specimens revealed the following five types of  $\text{ZnCO}_3$  (Table 1).

Type I smithsonite corresponds to rhombohedral, distinctly idiomorphic, and commonly zoned smithsonite crystals (Figs. 3f and 4a, b), mainly found in the samples from the +92 level of the Nebida mine but also in samples derived from deeper levels in the mines of the Iglesias Valley. The crystals generally fill vugs and cavities of the high-grade ore samples or coat their outer surface, forming shiny crystalline encrustations. These well-developed crystals range between 50 and  $400 \mu\text{m}$  in size, and the surfaces of the grains are always free from any evidence of corrosion. Locally, interspersed among the rhombohedra, rare whitish calcite crystals and globular iron oxides and iron hydroxides occur. The massive replacement ores (Fig. 4c, d, e) from Nebida, Monte Agruxiau, and Monteponi mines, which consist of aggregates of microcrystalline rhombohedral crystals barely visible in the scanning electron microscope, are considered to belong to Type I smithsonite.

Type II smithsonite is not very common and refers to polycrystalline microaggregates of smithsonite, commonly with curved and slightly rounded faces. These specimens have been sampled in the Mt. Agruxiau mine (Fig. 3g) and at Seddas Moddizzis (Cicillonis open pit). The crystal surfaces appear locally rough and corroded; mean crystal sizes are in the range of 200 to  $400 \mu\text{m}$ . This type of smithsonite coats irregular vugs in earthy, grayish, smithsonite masses.

Type III smithsonite, the so-called “rice grains” of Stara et al. (1996), has been observed in several specimens of red, earthy calamine from the Mount Agruxiau mine and dumps (Table 1). SEM study reveals that these forms consist mainly of microcrystalline aggregates but also of larger single elongated crystals (c-axis direction). Figure 4f shows a

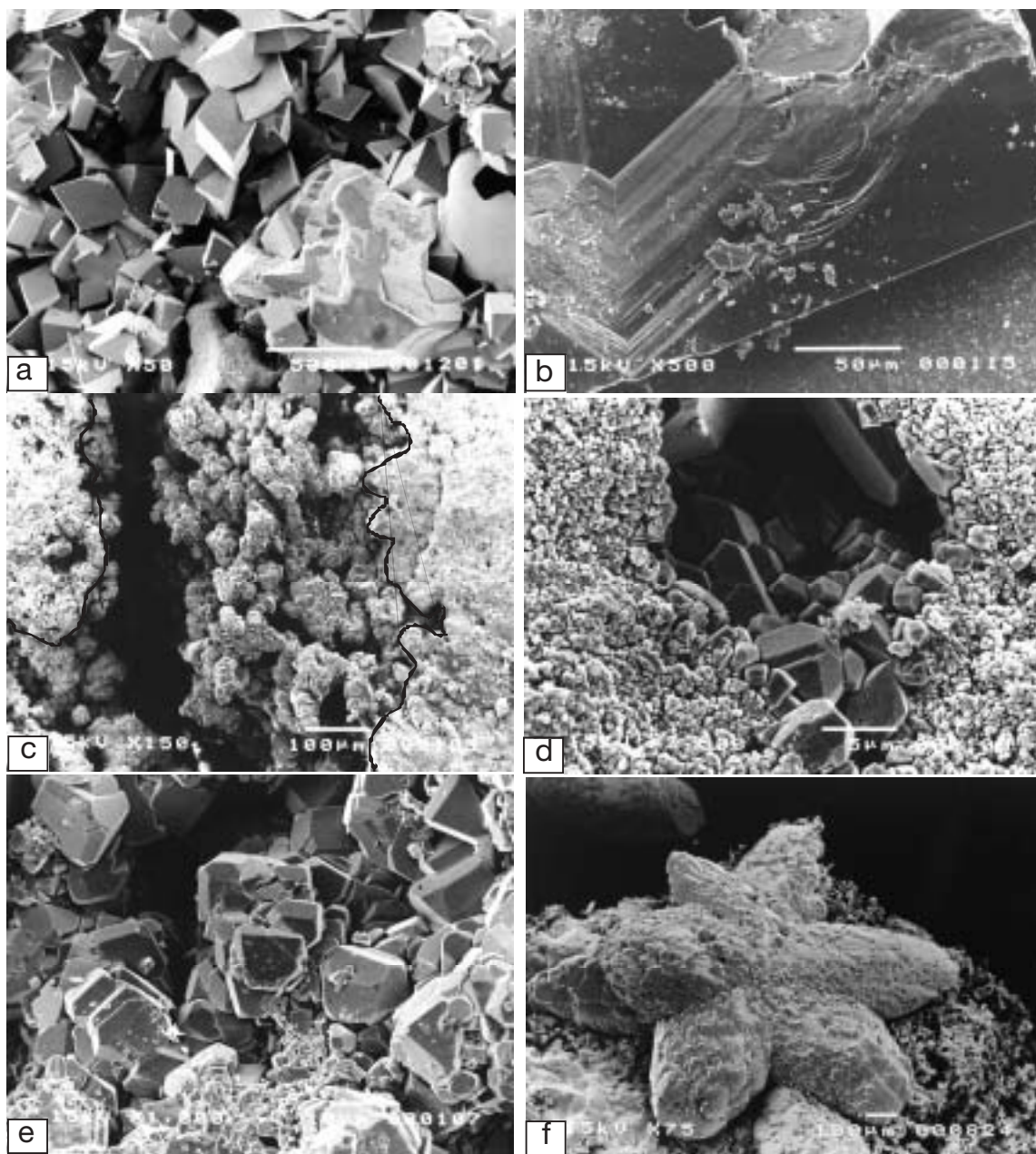


FIG. 4. SEM micrographs of types I and III Zn minerals at Nebida-Santa Margherita +92 level and at Mount Agruxiau. a. Nebida-Santa Margherita, 13-G: well developed rhombohedral crystals of smithsonite (type I). b. Same sample as in (a): enlargement of a zoned smithsonite crystal. c. Nebida-Santa Margherita, 48-Ga: massive (replacement) smithsonite grading to microcrystalline smithsonite (type I). d. Same sample as in (c): cavities in the massive smithsonite filled with hemimorphite crystals. e. Same sample as in (c): enlargement of microcrystalline smithsonite. f. Mount Agruxiau, 8-G: "rice grain" smithsonite aggregates (type III).

typical cluster of "rice grain" smithsonite whose grain dimension ranges from 1 mm to 250  $\mu\text{m}$ .

Type IV smithsonite consists of botryoidal aggregates of platy smithsonite microcrystals and is characteristic of the San Giovanni mine (Table 1). This type of smithsonite was also found in samples from the San Benedetto and Seddas Moddizis mines. SEM images (Fig. 5a) show that the globular aggregates are 600  $\mu\text{m}$  in size and contain platy surfaces corresponding to the  $\{1011\}$  cleavage.

Type V smithsonite is a variation of type IV, occurring in globular concretions without the typical platy surfaces (Fig. 5b). Locally, type V evolves to stalactitic forms hanging in karstic cavities in the vadose zone. These Zn carbonate phases seem to be fairly recent, because they have been found only in the upper levels of the mines together with green and blue aragonite concretions (Fig. 3h).

The stalactitic yellow-green smithsonite from the Nebida and Masua mines (Fig. 3d, e) is typical, but we could sample

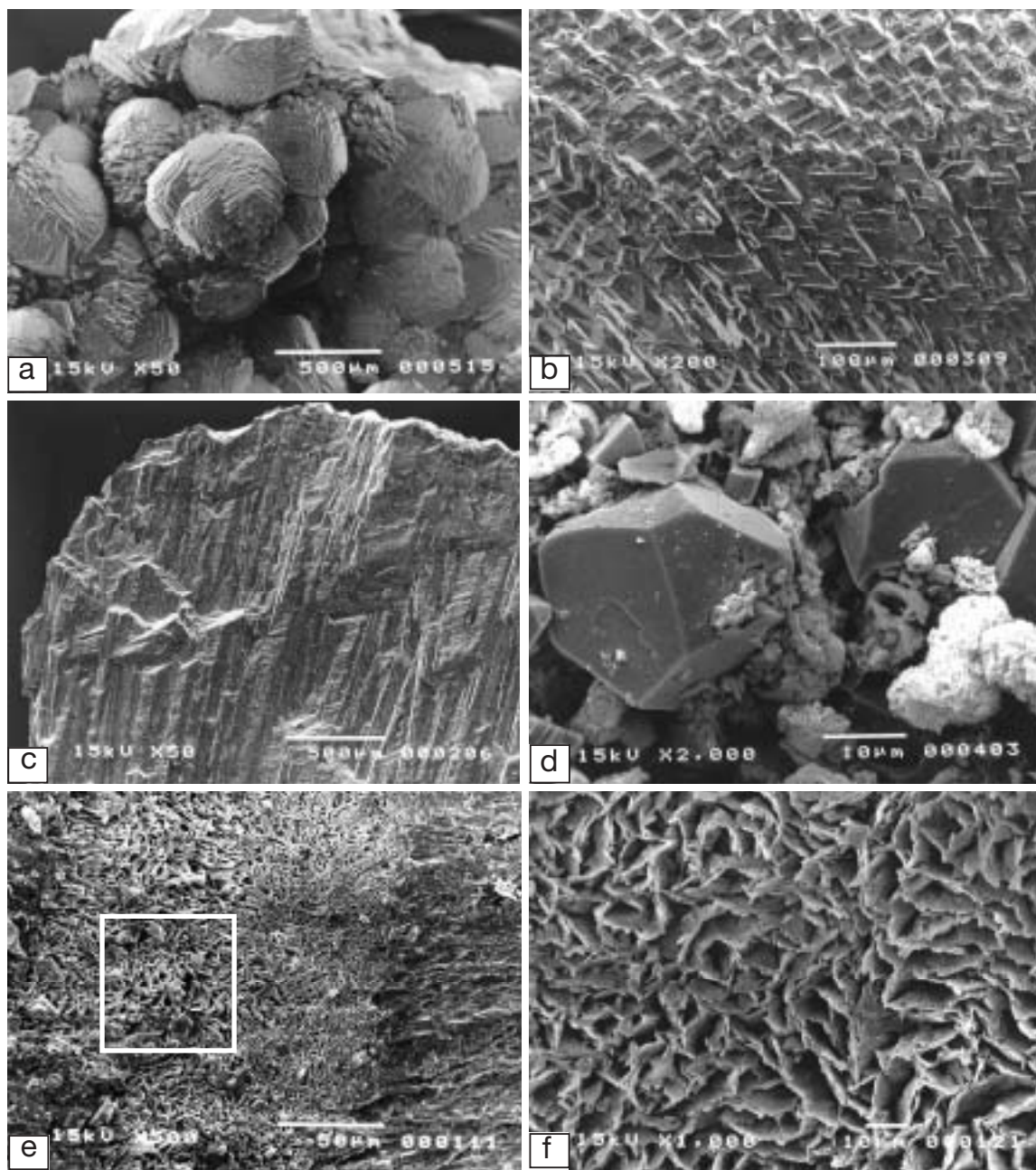


FIG. 5. SEM micrographs of type IV and V Zn minerals at Nebida-Canale San Giuseppe, Masua-Lanusei San Giovanni, and Monteponi-Cungiaus. a. Nebida-Canale San Giuseppe, 24-G: globular aggregates of platy smithsonite microcrystals (type IV). b. Masua-Lanusei, Sar-1: microcrystalline surface of the botryoidal Cd-rich smithsonite stalactite (type V). c. San Giovanni, 52-G: microfragment of white smithsonite stalactite (type V). d. Nebida, 13-Gb: hydrozincite (white concretions) filling pore space and replacing crystals of idiomorphic smithsonite. e. Monteponi-Cungiaus, Sar-2: gray concretionary smithsonite (type IV) on the right, grading to hydrozincite on the left. f. Enlargement of the square in Fig. 5e: typical scaly hydrozincite aggregate (Sar-3).

it only from a private collection. A white variety of these stalactites also occurred in the higher levels of the San Giovanni mine (Fig. 5c). They correspond to the mineral specimens once denominated “noble calamine” or “gel calamine” (Cavinato, 1952), a mineral variety known in the world of English-speaking mineral collectors as “turkey fat” smithsonite. Other varieties of smithsonite with a powdery (white to orange)

appearance (samples Sar1a and Sar1b) occur with type V smithsonite, but they are not crystalline.

A peculiar Fe-rich smithsonite, classified as monheimite (M-type), was sampled in the deeper part of the Montevecchio mine (Arburese district, about 30 km north of the area shown in Fig. 1), where a set of Zn-Cu-Pb veins cutting a lower Paleozoic slate formation was exploited near the Arbus

granite. This carbonate variety, analyzed for comparison, is a member of the siderite-smithsonite series that has a composition about midway between smithsonite and siderite (Palache et al., 1951; Zuffardi, 1952; Sitzia, 1965; Bak and Niec, 1978; Bak and Zabinski, 1981).

Several sets of X-ray powder-diffraction patterns were obtained for types I to V smithsonite. Their cell parameters differ slightly from the data quoted in the literature and range from  $a$  4.659(4) to 4.665(3) Å and  $c$  15.038(2) to 15.050(5) Å (Effenberger et al., 1981; Chang et al., 1996). Moreover, there is no direct correspondence between the morphology of the smithsonite crystals, their content in minor and trace elements, and their cell parameters. Microprobe analyses reveal quite homogeneous chemical compositions for all the smithsonites analyzed. The Zn content is in the range of 1.885 to 1.986 atoms per formula unit (apfu). Among the other trace elements, only  $\text{Ca}^{2+}$  reaches significant amounts (up to 0.09 apfu) in a few cases, suggesting an irregular distribution of  $\text{Ca}^{2+}$ . Fe and Mn can reach 0.024 and 0.012 apfu, respectively, and the Mg content is in the range 0.005 to 0.017 apfu. Traces of Cd have been detected only in the yellow stalactitic smithsonite of type V.

Hydrozincite is commonly associated with smithsonite. At the hand-specimen scale, hydrozincite commonly appears as whitish crustiform masses, locally growing directly on smithsonite crystals or smeared on cerussite. Locally hydrozincite seems to fill pore spaces between smithsonite crystals and even replace them (Fig. 5d). X-ray diffraction and energy-dispersive X-ray analyses show that their unit cells do not differ significantly from the JCPDS-ICDD data or from chemical analyses and that they are mostly close to the stoichiometric compositions. SEM micrographs of hydrozincite (Fig. 5e, f) show the typical scaly habit of these hydrous carbonates.

#### *Hemimorphite and cerussite*

Other supergene minerals associated with the Zn carbonates are hemimorphite and cerussite. Hemimorphite consists of idiomorphic crystals occurring as encrustations and open-space infill in massive hydrozincite (Monteponi) or as drusy encrustations growing on smithsonite surfaces (Fig. 4d). Two samples from the Mount Agruxiau and San Benedetto mines (Table 1) consist of tabular hemimorphite only. The anomalous abundance of hemimorphite in most calamine deposits in a predominantly limestone district suggests that silica was highly mobile during supergene alteration (Moore, 1972). Hemimorphite unit cell spacings are always around  $a$  8.365(8),  $b$  10.711(6) and  $c$  5.116(8) Å, similar to the values reported by McDonald and Cruickshank (1967). The EDS analyses of all the samples reveal homogeneous and practically stoichiometric chemical compositions, except for the traces of Cu found in the specimens from the Sa Duchessa mine, consistent with the alteration of Cu sulfides occurring in the primary orebody.

Cerussite occurs both in Nebida and Monteponi, commonly as whitish well-formed crystals (up to 0.3 mm in size) and as {110} twins, and locally as encrustations on small nuclei of galena. However, nodules of relict (or even supergene) galena are common in the residual deposits. Cerussite from the Monteponi mine occurs in aggregates of large crystals with the typical twinning; the average cell dimensions are  $a$

5.178(2),  $b$  8.497(1) and  $c$  6.139(3) Å, close to the structural parameters obtained from neutron diffraction refinement by Chevrier et al (1992). Most cerussite samples analyzed for the present work are close in composition to ideal  $\text{PbCO}_3$ . Minor amounts of  $\text{Ca}^{2+}$  and  $\text{Zn}^{2+}$  were also found as traces in Pb carbonates.

#### *Calcite and aragonite*

The crystallographic data of meteoric calcites show cell parameters close to  $a$  4.985(5) and  $c$  17.057(4) Å, similar to the structure refinement data of Effenberger et al. (1981). Hydrothermal scalenohedral calcite from the Masua mine shows only slightly different unit cell dimensions, with  $a$  4.980(2) and  $c$  17.051(2). All calcite samples are nearly pure  $\text{CaCO}_3$ ; only traces of Mg, Fe, and Mn were observed.

Aragonites, ranging from milky white to light green in color, have cell parameters of  $a$  4.960(2),  $b$  7.971(1), and  $c$  5.738(3) Å, in agreement with the data of Dal Negro and Ungaretti (1971). On the whole they have a stoichiometric composition, and only trace amounts of Sr (in some EPM point analyses) and Cu (in the green specimen from the San Giovanni mine) are found.

### Isotopic Geochemistry

#### *Zn and Pb carbonates*

The results of the oxygen and carbon isotope measurements are presented in Table 1 and depicted in Figure 6. The two analytical techniques yield comparable results for smithsonite with deviations usually less than  $\pm 0.2$  per mil (Table 1). Smithsonites display a small range in  $\delta^{18}\text{O}$  values from 25.5 to 28.9 per mil and an average value of  $27.4 \pm 0.9$  per mil ( $1\sigma$ ,  $n = 26$ ). There is no systematic difference in  $\delta^{18}\text{O}$  values from various deposits or between petrographic types (Fig. 6). This points to a relatively uniform isotopic composition of the oxidizing fluid and constant temperatures of smithsonite crystallization (Gilg et al., 2001). The Fe smithsonite ("monheimite") from Montevecchio (sample 5-G), however, has a much lower  $\delta^{18}\text{O}$  value (21.0‰) compared with all other smithsonites (Fig. 6). This value suggests either higher crystallization temperatures or formation from a more  $^{18}\text{O}$ -depleted fluid. In contrast to oxygen,  $\delta^{13}\text{C}$  values of smithsonite range from  $-10.4$  to  $-0.6$  per mil (Fig. 6). The botryoidal and stalactitic smithsonite (type V) are characterized by high  $\delta^{13}\text{C}$  values of  $-3.9$  to  $-0.6$  per mil, whereas all other types of smithsonite have much lower  $\delta^{13}\text{C}$  values ( $< -3.9\text{‰}$ ). We note also that the range of  $\delta^{13}\text{C}$  values of smithsonite is comparable to the range of  $\delta^{13}\text{C}$  values of Mesozoic to Recent low-temperature calcite or aragonite from the same area (see below). Both oxygen and carbon isotope values of hydrozincite fall within the range of values recorded for smithsonites. Secondary Pb carbonate minerals have low  $\delta^{18}\text{O}$  values, 17.6 to 21.1 per mil, and  $\delta^{13}\text{C}$  values of  $-11.9$  to  $-7.2$  per mil for cerussite and phosgenite, respectively (Fig. 6).

#### *Ca carbonates*

Calcite crystals and concretions that are associated with calamine ore, most of them paragenetically slightly younger than smithsonites, have relatively low  $\delta^{13}\text{C}$  values of  $-11.3$  to  $-9.2$  per mil and consistent  $\delta^{18}\text{O}$  values of  $\sim 25.1 \pm 0.5$  per mil

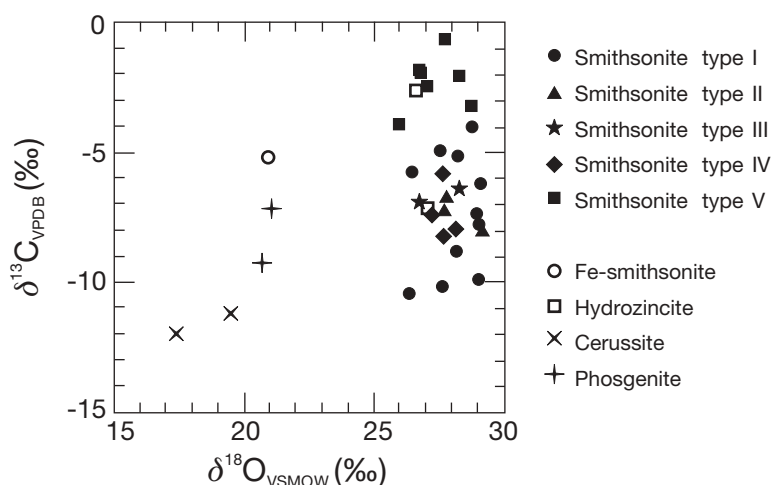


FIG. 6. Plot of  $\delta^{13}\text{C}$  vs.  $\delta^{18}\text{O}$  for various Pb and Zn carbonates (cerussite, phosgenite, hydrozincite, and smithsonite) from calamine ores from southwest Sardinia. Smithsonite types (petrographic groups) are described in the text.

(Fig. 7). The isotopic compositions of these calcite are clearly distinct from those of hydrothermal calcite and dolomite in the altered wall rock, as well as from calcite of the internal sediments in Mesozoic (?) hydrothermal paleokarst, which have lower  $\delta^{18}\text{O}$  (15.1–23.7‰) and higher  $\delta^{13}\text{C}$  values (–3.5 to –0.7‰) (Fig. 7). The measured values of these hydrothermal carbonates are comparable to previous measurements

made by Boni et al. (2000) and DeVivo et al. (1987), although some of our  $\delta^{13}\text{C}$  values appear slightly lower. The  $\delta^{18}\text{O}$  values of calcites associated with calamine ore, however, are similar to those of low-temperature meteoric carbonates in southwest Sardinia (caliche, travertines, and speleothems) from Triassic to Recent (Fig. 7). The  $\delta^{18}\text{O}$  values of the majority (six samples) of these low-temperature calcites and

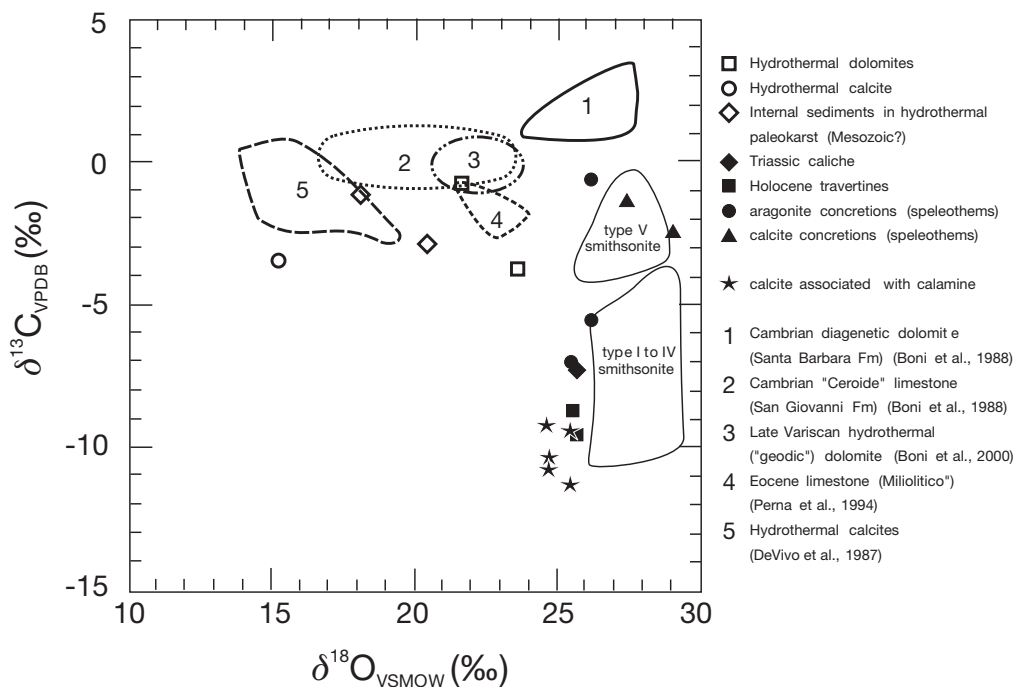


FIG. 7. Plot of  $\delta^{13}\text{C}$  vs.  $\delta^{18}\text{O}$  for Ca ( $\pm$ Mg) carbonates (calcite, aragonite, and dolomite) from southwest Sardinia. The stars denote calcite associated with calamine ore. Open symbols represent hydrothermal carbonates, whereas filled symbols indicate freshwater low-temperature carbonates such as caliche, travertine, and speleothems ranging in age from Triassic to sub-Recent. The fields 1 to 3 depict the isotope compositions of wall rocks of calamine ores (from Boni et al., 1988, 2000). The range of isotope compositions of Eocene marine limestones (field 4, from Perna et al., 1994) and hydrothermal scalenohedral calcites (field 5, from De Vivo et al., 1987) are shown for comparison.

aragonites cluster around  $26.0 \pm 0.5$  per mil. Only two samples, a calcite concretion from a Quaternary bone bed at Nebida (sample 66-G) and a calcite stalactite from the San Giovanni cave (sample 21-G), have somewhat higher  $\delta^{18}\text{O}$  values (27.5 and 29.1‰, respectively). These values could be related either to lower temperatures or, more likely, to the effect of evaporation (e.g., Schwarcz, 1986; Lohmann, 1988).

The  $\delta^{13}\text{C}$  values of the low-temperature meteoric Ca carbonates show a considerable range from  $-8.7$  to  $-0.6$  per mil (Fig. 7). The values most depleted in  $^{13}\text{C}$  are related to Holocene travertines, Triassic caliche, and one concretion from Seddas De Daga cave, whereas most stalactites forming in the vadose zone have high  $\delta^{13}\text{C}$  values.

## Discussion

### Geologic controls on calamine formation

Observations at the ore deposit scale, combined with data from the literature and from old mine reports, confirm that calamine in Sardinia formed both in situ, from the replacement of primary sulfides and carbonates and, to a much lesser extent, accumulated detritally in a network of karstic cavities. However, the relative roles of lithology and permeability contrasts, recent faults and fractures, proximity of older paleokarstic structures, and the presence of late-Variscan hydrothermally dolomitized host rocks are still not completely understood. Probably one of the most important

factors contributing to the deep oxidation was the vertical dip of primary sulfide ores coupled with a strong schistosity in the Cambrian carbonate rocks acquired during Variscan tectonics, which made the strata-bound primary sulfides accessible to deep infiltration and circulation of meteoric waters. Through oxidation of sulfide and the resulting increased acidity, these waters also dissolved the host carbonate rocks. As a result, most carbonate rocks in the Iglesiente area show enhanced corrosion at various depths in the karstic system, resulting in a permeability network of huge interconnecting cavities referred to by De Waele et al. (2001) as “hyperkarst.” Some of the karst cavities have maximum sizes higher than 40 m. Figure 8 shows the distribution of the calamine ore in the evolution of a “hyperkarstic” profile; most of the ore is located between the meteoric vadose (percolation) and the epiphreatic (oscillation) zones.

In southwest Sardinia, the level of oxidation is highly variable in different areas of the mining district. These differences may be related to several distinct phases of block faulting that displaced mature oxidation profiles, initiated in the Cambrian carbonate rocks following post-Variscan peneplanation (Boni et al., 2001). These vertical tectonic movements occurred during both the Tertiary and Quaternary periods. A more recent reactivation of the former alteration profiles has been observed locally, leading to the formation of the stalactitic formations of the Masua and San Giovanni mines (see below), as well as the late botryoidal crusts and crystals. These

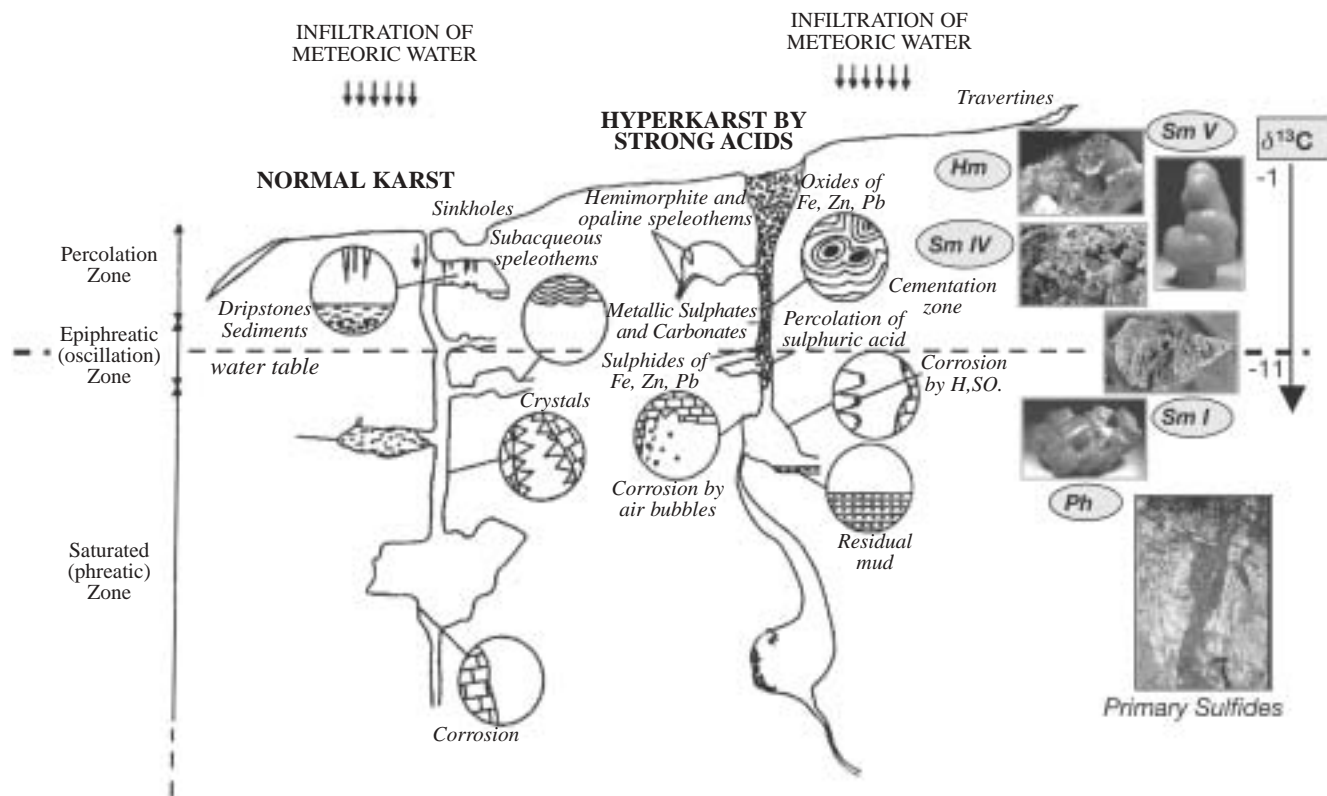


FIG. 8. Geologic sketch (modified from De Waele et al., 2001) of the “hyperkarstic” environment in southwest Sardinia, with the position of the different types of calamine ore in relation to vadose and phreatic zones. The arrow on the right of the figure shows the range of  $\delta^{13}\text{C}$  values, from approximately  $-11$  to  $0$  per mil, recorded in the different morphologic smithsonite types from the percolation zone downward. Hm = Hemimorphite, Ph = Phosgenite, Sm I = Smithsonite type I, Sm IV = Smithsonite type IV, Sm V = Smithsonite type V.

consist of both Zn carbonates and silicates and coat the earlier-deposited massive ores.

The smithsonite stalactites and the botryoidal crusts, as well as hemimorphite and some hydrozincite concretions, appear to be restricted to the vadose zone of the paleokarstic network. In contrast, the other smithsonite generations record a more complex history of replacement following the dissolution of limestone and dolostone by acid solutions generated during oxidation of the primary sulfides.

#### *Mineral paragenesis and physicochemical conditions of calamine formation*

The mineral assemblage anglesite-cerussite-phosgenite is restricted to secondary oxidation zones in contact with galena, whereas the typical hemimorphite-smithsonite-goethite (calamine) ores occur in sulfide-free zones. However, smithsonite, hydrozincite, and hemimorphite in the calamine ore are not always cogenetic, as indicated both from mine zonation and petrography. In fact, at least some smithsonite (types I, IV, and V) started to precipitate earlier than types II and III, following the paragenetic sequence smithsonite → hydrozincite → hemimorphite observed in a few samples. Type I smithsonite appears to replace both limestone and hydrothermal dolomite in several mines (e.g., Nebida, Monteponi). The early smithsonite can also be replaced by hydrozincite at the border of the crystals and along fractures (Fig. 5d), whereas botryoidal hemimorphite overgrows both phases or occurs as fine elongated crystals in vugs (Fig. 4d). Smithsonites of type II and III, coating the surface of gossans or growing in fractures, belong to more recent phases of deposition, whereas the smithsonite stalactites of type V seem to be still forming through the present karstic network.

The stability of supergene Zn and Pb minerals in terms of physicochemical parameters, such as pH,  $P_{\text{CO}_2}$ , and concentration of Zn and Pb species or silica in solution, have been discussed in detail by Takahashi (1960), Mann and Deutscher (1980), Sangameshwar and Barnes (1983), Ingwersen (1990), and Williams (1990). Relatively low pH conditions (~4–6 depending on  $P_{\text{CO}_2}$  and sulfate activity) are indicated for anglesite-cerussite-phosgenite associations, whereas smithsonite-hemimorphite-hydrozincite ores are stable under intermediate to high pH values buffered by the carbonate host rocks. The predominance of smithsonite as compared with (in most cases very late) hydrozincite suggests relatively high  $P_{\text{CO}_2}$  conditions ( $>10^{1.41}$  atm) in excess of atmospheric  $\text{CO}_2$  partial pressures (Williams, 1990). These conditions could have been maintained by neutralization of the oxidizing solutions by the carbonate host rocks or by decrease of  $P_{\text{CO}_2}$  during late stage hydrozincite formation at the expense of smithsonite.

#### *Isotopic geochemistry*

*Temperature of calamine formation:* There are no published experimental determinations of smithsonite-water isotopic fractionation. However, the temperature dependence of oxygen isotope fractionation between smithsonite and water was calculated by Golyshev et al. (1981) using a statistical thermodynamic model and more recently by Zheng (1999) using the modified increment method. The  $1000 \ln \alpha_{\text{smithsonite-water}}$  values calculated by Golyshev et al. (1981) are up to 7 per mil lower

at temperatures below 50°C than those of Zheng (1999). We note a similar discrepancy between the two approaches for the cerussite-water fractionation. A recent experimental determination of the cerussite-water fractionation between 20° and 65°C by Melchiorre et al. (2001) yields similar or even slightly larger  $1000 \ln \alpha$  values than those predicted by Zheng (1999). We therefore use the expression given by Zheng (1999):

$$1000 \ln \alpha_{\text{smithsonite-water}} = 4.27 \cdot 10^6/T^2 - 4.56 \cdot 10^3/T + 1.73$$

with T in Kelvin for our temperature estimates of smithsonite formation.

In order to calculate the temperature of smithsonite formation, the isotopic composition of the oxidizing water has to be known as well. Present-day meteoric waters in the Iglesias mining district have  $\delta^{18}\text{O}$  values of  $-6.5 \pm 1$  per mil (Civita et al., 1983; DeVivo et al., 1987; Cidu et al., 2001). Similar values of  $-7.0$  to  $-4.5$  per mil have been calculated for the low-salinity meteoric hydrothermal fluids that precipitated scalenohedral calcites in karstic caves of the Masua mine, using combined oxygen isotope data of calcites and fluid inclusion measurements (DeVivo et al., 1987). We note that the oxygen isotope compositions of low-temperature, freshwater Ca carbonates (caliche, travertine, and speleothems) from Triassic to Recent are similar in southwest Sardinia (Friedman and O'Neil, 1977). This similarity may indicate that the oxygen isotope composition of local meteoric waters has not changed significantly throughout the Mesozoic and Cenozoic. Thus, assuming a  $\delta^{18}\text{O}$  value of the oxidizing waters of  $-6.5$  per mil, a temperature range of 20° to 35°C is calculated for the crystallization of smithsonite in Sardinian calamine ore (Fig. 9). Using the same isotopic composition of water and the cerussite-water fractionation equation of Melchiorre et al. (2001), our pure cerussite sample (10-G) yields a comparable temperature of 35°C. Much lower temperatures of 5° to 10°C are, however, calculated for the calcites associated with calamine ore using

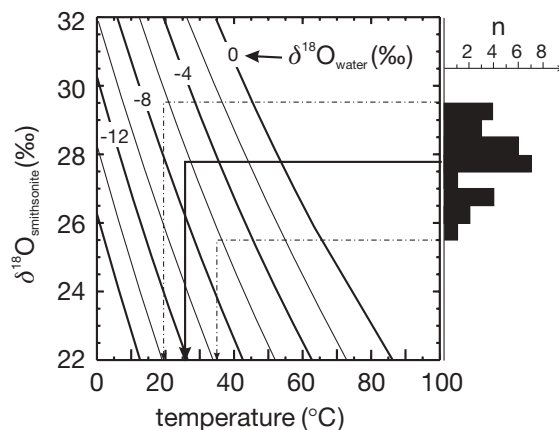


FIG. 9. Graphical representation of oxygen isotope equilibrium curves between smithsonite and water according to Zheng (1999), calculated for different  $\delta^{18}\text{O}_{\text{H}_2\text{O}}$  values as a function of temperature. The histogram to the right shows the oxygen isotope composition of smithsonites from southwest Sardinia. Temperature estimates for smithsonite formation are based on a  $\delta^{18}\text{O}_{\text{VSMOW}}$  value of  $-6.5$  per mil for the local (paleo)meteoric water.

the same isotopic composition of water and the calcite-water fractionation equation of O'Neil et al. (1969). Although the discrepancies between temperatures indicated by Zn and Pb carbonates and those deduced from Ca carbonates alone may be related to changing isotopic compositions of the meteoric water or to uncertainties in the isotope fractionation factors involved, they could also represent real changes in temperatures during calamine formation. High temperatures of 30° to 70°C during formation of secondary oxidized Cu and Pb carbonates from sulfide ores have been documented by Melchiorre et al. (1999, 2000, 2001) and Melchiorre and Williams (2001) using oxygen isotopes. Furthermore, Melchiorre and Williams (2001) also documented a temperature drop of ~20°C from crystallization of azurite and malachite to late-stage calcites during the oxidation of the Great Australia deposit in Queensland, Australia. Because most calcites associated with calamine ores of Sardinia formed late in the paragenetic sequence, they could have formed at lower temperatures and much later than smithsonite. Other measured freshwater calcites and aragonites (such as travertines, speleothems) are not in paragenetic contact with the Zn carbonates.

*Source of carbon:* The wide range of carbon isotope values of smithsonites, as well as hydrozincites, indicates at least two sources of carbon: <sup>13</sup>C-depleted, reduced organic carbon and <sup>13</sup>C-enriched, marine carbonate carbon. The carbonate-bearing wall rocks of calamine ores, such as Cambrian diagenetic dolostones of the Santa Barbara Formation, Cambrian limestone of the San Giovanni Formation, or late Variscan pervasive hydrothermal dolomite (Fig. 7), are all characterized by high  $\delta^{13}\text{C}$  values ( $\delta^{13}\text{C} = 0 \pm 2\text{‰}$ ) and could be the source of <sup>13</sup>C-enriched carbon. The dissolution of marine limestone and dolostone of origin would have been promoted by acid solutions generated during oxidation of the primary sulfides (e.g., Williams, 1990). The absence of any correlation between carbon and oxygen isotope values suggests that direct participation of Mediterranean seawater during oxidation, as hypothesized by Zuffardi (1952), as a source for the <sup>13</sup>C-enriched component in smithsonite can be excluded. The <sup>13</sup>C-depleted source of carbon is most probably organic matter dominated by C3 plants in the soil zone (e.g., Lohmann, 1988). Low carbon isotope values ( $\delta^{13}\text{C} = -10 \pm 1\text{‰}$ ) are also found in Holocene travertine and in calcite associated with calamine ore (Fig. 7). Similar values, however, were also measured by DeVivo et al. (1987) in late-stage cave carbonates formed at ambient temperatures in the phreatic zone at the Masua mine that are not directly associated with calamine ore. The  $\delta^{13}\text{C}$  values of  $\text{HCO}_3^-$  in present-day ground waters in the mining area scatter around -11 per mil (DeVivo et al., 1987) and are thus dominated by the same <sup>13</sup>C-depleted carbon source.

Both Zn carbonates (smithsonites and hydrozincites) and low-temperature calcites and aragonites from the Iglesias mining area have an almost identical and quite wide range of  $\delta^{13}\text{C}$  values, approximately -11 to 0 per mil. This range is interpreted to indicate that both sources of carbon participated in the formation of smithsonite and calcite and that the latter minerals have similar carbon isotope fractionation factors. The <sup>13</sup>C-enriched source (marine carbonate wall rocks) seems to have dominated during formation of botryoidal and stalactitic smithsonite (type V) that clearly formed in the

vadose zone, whereas all other types of smithsonite (from I to IV), ranging from euhedral crystals of various types to massive replacements that formed in the epiphreatic zone, have much lower  $\delta^{13}\text{C}$  values. This observation is surprising, because some of the massive smithsonites (type I) with low  $\delta^{13}\text{C}$  values directly replaced <sup>13</sup>C-enriched carbonates, and this probably indicates high water/rock ratios. Also, our few carbon isotope analyses of euhedral Pb carbonate crystals (cerussite and phosgenite) show a <sup>13</sup>C-depleted signature ( $\delta^{13}\text{C} = -12$  to  $-7\text{‰}$ ), consistent with the smithsonite and hydrozincite data.

*Source of waters responsible for sulfide oxidation:* Many mines in the Iglesias district that contain nonsulfide ores are located in a belt close to the Mediterranean sea, and the exploitation reached well b.s.l.. There is an extensive literature on possible seawater circulation in the hydrologic system of western Iglesias, the effects of which were considered to be of utmost importance in the Monteponi and San Giovanni carbonate blocks (Zuffardi, 1952; Cidu et al., 2001). In addition, after the closure of the mine at Monteponi, the ingress of seawater and formation of mixed marine-meteoric waters was observed (Cidu et al., 2001). Cl-rich oxidation minerals, such as phosgenite ( $\text{Pb}_2\text{Cl}_2\text{CO}_3$ ), which is found in some of the mines along the coastal belt but especially at Monteponi, may indicate that seawater played a role in the formation of these minerals.

However, the large variation of carbon isotope values of smithsonites, combined with the restricted range of oxygen isotope values, suggests that only one type of water was involved in oxidation. The observed pattern in a C-O isotope plot (Fig. 7) strongly resembles the "meteoric calcite line" of Lohmann (1988) (e.g., a possible "meteoric smithsonite line"). Reasonable temperatures (<40°C) and geologic conditions, especially for the formation of smithsonite stalactites, are indicated only by assuming deposition from meteoric waters. The typical calamine ores of southwest Sardinia are related to deep continental weathering involving meteoric waters.

### Timing

The time constraints for the deposition of the calamine ores in southwest Sardinia are still unclear, owing to multiple oxidation events through time and the complex paragenesis of newly formed Zn carbonates. However, the most reliable time span in which both tectonic and climatic conditions were favorable for the formation of most of the mineral deposits ranges from middle Eocene—which was the emersion phase in most of Sardinia, followed by lateritization of the Paleozoic lithotypes, deep karstification, and deposition of the continental Cixerri Formation—to Plio-Pleistocene—when a tensional tectonic phase was responsible for the differentiated uplift of distinct sectors of the Paleozoic basement.

In fact, it has been observed that in most calamine deposits occurring in the Iglesias carbonate rocks, the lowest level of oxidation is displaced in the various areas at very different levels in relation to the recent water table (Fig. 2), confirming the fossil age of the oxidation phenomena. A period of generalized sea level drop in the Mediterranean realm during the Messinian could also have played an important role in calamine formation. A problem, though, is the well-known arid climatic conditions prevailing during Messinian time,

which may have prevented the development of an extensive karstic network in the area.

Extension in the early Pleistocene seems to have been the latest event in Sardinia capable of causing differentiated uplift of the Paleozoic fault blocks. In the southwestern region, these rocks consist of sulfide-hosting Cambrian carbonate rocks, which had already undergone a powerful oxidation associated with the development of a microkarstic and macrokarstic network that originated during long and repeated periods of emersion.

Further multiple reactivations of the weathering profiles in southwest Sardinia, especially within the warm interglacial periods of the Quaternary, cannot be excluded. The botryoidal and stalactitic smithsonites deposited in the vadose zone, as well as many unrooted "earthy" calamine deposits occurring in dolines, may be related to these more recent phenomena.

### Conclusions

The main economic minerals of the "calamine" type deposits in southwest Sardinia, consist of Zn (hydroxy-)carbonates and silicates (smithsonite, hydrozincite, and hemimorphite) associated with Fe and Mn oxy(hydroxides) and residual clays. The mineralization is considered to be the result of in situ oxidation and replacement, locally with limited transport, of the primary sulfide phases, brought about by meteoric fluids circulating in a deep karstic network in Cambrian carbonate rocks. There is strong evidence that the oxidation profiles and related nonsulfide mineral deposits evolved throughout the late Tertiary and were later displaced (and eventually rejuvenated) by younger block tectonics.

Smithsonite occurs in the calamine ores in five morphologic forms, from perfectly crystalline to cryptocrystalline botryoidal. These forms are related to the various depositional environment of smithsonite within the karstic system. The oxygen isotope compositions of smithsonite are uniform, and no systematic differences exist in  $\delta^{18}\text{O}$  values from various deposits or between petrographic types. This uniformity points to a relatively uniform isotopic composition of the oxidation fluid and constant temperatures of smithsonite crystallization, within the range 20° to 35°C, similar to the temperature calculated for cerussite (35°C). Much lower temperatures of 5° to 10°C have been calculated for the freshwater calcites associated with calamine.

In contrast, the wide range of carbon isotope values measured in Zn carbonates indicates participation of at least two sources of carbon:  $^{13}\text{C}$ -depleted reduced organic carbon (soils?) and  $^{13}\text{C}$ -enriched marine carbonate (Cambrian host rock) carbon. The  $^{13}\text{C}$ -enriched source seems to dominate during formation of type V smithsonite that formed in the vadose zone, whereas smithsonites from types I to IV formed in the epiphreatic zone and have much lower  $\delta^{13}\text{C}$  values. Zn carbonates and low-temperature Ca carbonates have an almost identical range of  $\delta^{13}\text{C}$  values from approximately -11 to 0 per mil. This similarity indicates similar sources of carbon and similar carbon isotope fractionation factors for smithsonite and calcite. Moreover, the absence of a correlation between carbon and oxygen isotope values suggests that direct participation of Mediterranean seawater during oxidation can be excluded.

At the moment (2003) only very limited geologic constraints exist with regard to the timing of bulk nonsulfide mineralization in southwest Sardinia, a problem that could also

have interesting implications for exploration of this type of ore in similar environments elsewhere. Therefore, it remains a priority to obtain a direct age of the oxidation phenomena, either by paleomagnetic methods or by use of radiogenic isotope systems, such as  $^{40}\text{Ar}/^{39}\text{Ar}$  or U-Th-He on K-Mn oxides.

### Acknowledgments

The authors thank the IGEA Company (Iglesias, Sardinia) for having granted access to their properties and R. Sarritzu for help and discussions. Special thanks are expressed to S. Pretti, G. Manunta, and E. Cocco for providing samples from their collections and to A. Canzanella (Centro Interdipartimentale Strumentale Analitico Geomineralogico, Università di Napoli) for assistance with SEM-EDS analyses. We acknowledge the help of U. Struck with stable isotope analyses at the Bayerische Paläontologische Staatssammlung, München. Thanks are also due to two *Economic Geology* referees (J. Gregg and G. Beau-doin) and to M. Hannington and D. Sangster for careful editing.

### REFERENCES

- Annels, A.E., O'Donovan, G., and Bowles, M., 2003, New ideas concerning the genesis of the Angouran Zn-Pb deposit, NW Iran [abs.]: Mineral Deposits Studies Group AGM, 26th, University of Leicester, United Kingdom, 2003, Abstracts, p. 11-12.
- Assorgia, A., Barca, S., Cocozza, T., Decandia, F.A., Fadda, A., Gandin, A., and Ottelli, L., 1992, Characters of the Cenozoic sedimentary and volcanic succession of western Sulcis (SW Sardinia), in Carmignani, L., and Sassi, F.P., eds., Contribution to the geology of Italy with special regard to the Palaeozoic basement: International Geological Correlation Program 276 Newsletter, v. 5, p. 17-20.
- Aversa, G., Balassone, G., Boni, M., and Amalfitano, C., 2002, The mineralogy of the "calamine" ores in SW Sardinia (Italy): Preliminary results: *Periodico di Mineralogia*, v. 71, p. 1-18.
- Bak, B., and Niec, M., 1978, The occurrence of monheimite in the Boleslaw Zn-Pb ore deposits near Olkusz: *Mineralogica Polonica*, v. 9, p. 123-128.
- Bak, B., and Zabinski, W., 1981, On the continuity of the solid solution series smithsonite-siderite: *Mineralogica Polonica*, v. 12, p. 75-80.
- Bechstädt, Th., and Boni, M., eds., 1994, Sedimentological, stratigraphical and ore deposits field guide of the autochthonous Cambro-Ordovician of southwestern Sardinia: Servizio Geologico d'Italia Memorie Descrittive Carta Geologica d'Italia, v. XLVIII, 434 p.
- Billows, E., 1941, I minerali della Sardegna ed i loro giacimenti: *Rendiconti Università di Cagliari*, p. 331-335.
- Boland, M.B., Kelly, J.G., and Schaffalitsky, C., 2003, The Shaimerden supergene zinc deposit, Kazakhstan: *Economic Geology*, v. 98, p. 787-795.
- Boni, M., 1985, Les gisements de type Mississippi Valley du sud ouest de la Sardaigne (Italie): Une synthèse: *Chronique Recherches Minières BRGM* 489, p. 7-34.
- Boni, M., Iannace, A., and Pierre, C., 1988, Stable isotopes in the Lower Cambrian ore deposits and their host rocks in SW Sardinia: *Isotope Geoscience*, v. 72, p. 267-282.
- Boni, M., Iannace, A., Köppel, V., Hansmann, W., and Früh-Green, G., 1992, Late to post-Hercynian hydrothermal activity and mineralization in SW Sardinia: *Economic Geology*, v. 87, p. 2113-2137.
- Boni, M., Iannace, A., and Balassone, G., 1996, Base metal ores in the lower Palaeozoic of south-western Sardinia, in Sangster, D.F., ed., Carbonate-hosted lead-zinc deposits: Society of Economic Geologists Special Publication 4, p. 18-28.
- Boni, M., Parente, G., Bechstädt, Th., De Vivo, B., and Iannace, A., 2000, Hydrothermal dolomites in SW Sardinia (Italy): Evidence for a widespread late-Variscan fluid flow event: *Sedimentary Geology*, v. 131, p. 181-200.
- Boni, M., Iannace, A., Villa, I.M., Fedele, L., and Bodnar, R., 2001, Multiple fluid-flow events and mineralizations in SW Sardinia: A European perspective, in Cidu, R., ed., Water-Rock Interaction 2001: Villasimius, Lisse, The Netherlands, Balkema, Proceedings, v. 1, p. 673-676.
- Boni, M., Aversa, G., Balassone, G., and Gilg, H.A., in press, The Zn-Pb ore deposits in SW Sardinia (Italy): From sulfides to "calamine," in Andrew, C.J., Ashton, J.H., Boland, M.B., Earls, G., Kelly, J., and Stanley, G.A., eds., The geology and genesis of Europe's major base metal deposits: Irish Association for Economic Geology.

- Bonifazi, G., and Massacci, P., 1987, Characterization of oxidized zinc (calamine) ores by scanning electron microscopy and electron microprobe analysis: *Scanning Microscopy*, v. 1, p. 73–83.
- Borg, G., Kärner, K., Buxton, M., Armstrong, R., and Merwe, Schalk W. v.d., 2003, Geology of the Skorpion supergene zinc deposit, southern Namibia, *ECONOMIC GEOLOGY*, v. 98, p. 749–771.
- Carmignani, L., Cherchi, A., and Ricci, C.A., 1989, Basement structure and Mesozoic-Cenozoic evolution of Sardinia, in Boriani, A., Bonafede, M., Piccardo G.B., and Vai, G.B., eds., *The lithosphere in Italy: Accademia Nazionale dei Lincei*, p. 63–92.
- Carmignani, L., Carosi, R., Di Pisa, A., Gattiglio, M., Musumeci, G., Oggiano, G., and Pertusati, P.C., 1994, The Hercynian chain in Sardinia: *Geodinamica Acta*, v. 5-4, p. 217–233.
- Cavinato, A., 1952, I fenomeni di ossidazione nelle miniere dell'Iglesiente in Sardegna: *Resoconti Sedute Associazione Mineraria Sarda*, v. 57, p. 9–18.
- Chang, L.L.J., Howie, R.A., and Zussman, J., 1996, Rock-forming minerals. Non-silicates: v. 5B, London, Longman, 383 p.
- Cherchi, A., and Montadert, L., 1982, The Oligo-Miocene rift of Sardinia and the early history of the western Mediterranean basin: *Nature*, v. 298 (5876), p. 736–739.
- Chevrier, G., Giester, G., Heger, G., Jarosh, D., Wildner, M., and Zemann, J., 1992, Neutron single-crystal refinement of cerussite,  $PbCO_3$ , and comparison with other aragonite-type carbonates: *Zeitschrift Kristallographie*, v. 199, p. 67–74.
- Cidu, R., Biagini, C., Fanfani, L., La Ruffa, G., and Marras, I., 2001, Mine closure at Monteponi (Italy): Effect of the cessation of dewatering on the quality of shallow groundwater: *Applied Geochemistry*, v. 16, p. 489–502.
- Civita, M., Coccozza, T., Forti, P., Perna, G., and Turi, B., 1983, Idrogeologia del bacino minerario dell'Iglesiente: *Memorie Istituto Italiano Speleologia*. Ser. II, v. 2, p. 1–137.
- Dal Negro, A., and Ungaretti, L., 1977, Refinement of the crystal structure of aragonite: *American Mineralogist*, v. 56, p. 995–998.
- De Vivo, B., Maiorani, A., Perna, G., and Turi, B., 1987, Fluid inclusion and stable isotope studies of calcite, quartz and barite from karstic caves in the Masua mine, south-western Sardinia, Italy: *Chemie der Erde*, v. 46, p. 259–273.
- De Waele, J., Forti, P., and Perna, G., 2001, Hyperkarstic phenomena in the Iglesias mining district (SW Sardinia), in Cidu, R., ed., *Water-Rock Interaction 2001: Villasimius, Lisse, The Netherlands, Balkema, Proceedings*, v. 1, p. 619–622.
- Effenberger, H., Mereiter, K., and Zemann, J., 1981, Crystal structure refinement of magnesite, calcite, rhodocrosite, siderite, smithsonite and dolomite, with discussion on some aspects of the stereochemistry of calcite-type carbonate: *Zeitschrift Kristallographie*, v. 156, p. 233–243.
- Friedman, I., and O'Neil, J.R., 1977, Compilation of stable isotope fractionation factors of geochemical interest: *U.S. Geological Survey Professional Paper 440-KK*, p. 1–12.
- Gilg, H.A., Aversa, G., and Boni, M., 2001, A stable isotope study of smithsonite with application to Pb-Zn deposits of SW Sardinia, Italy: *EUG*, 11th, Strasbourg, p. 515.
- Gilg, H.A., Allen, C., Balassone, G., Boni, M., and Moore, F., in press a, The 3-stage evolution of the Angouran Zn "oxide"-sulfide deposit, Iran: *Mineral Exploration and Sustainable Development, Biennial SGA Meeting*, 7th, Athens, Greece, 2003.
- Gilg, H.A., Struck, U., Vennemann, T., and Boni, M., in press b, Phosphoric acid fractionation factors for smithsonite and cerussite between 25 and 72°C: *Geochimica Cosmochimica Acta*.
- Golyshev, S.I., Padalko, N.L., and Pechekin, S.A., 1981, Fractionation of stable oxygen and carbon isotopes in carbonate systems: *Geokhimiya*, v. 10, p. 1427–1441.
- Groves, I.M., and Carman, C.E., 2003, Geology of the Beltana willemite deposit, Flinders Ranges, South Australia, *ECONOMIC GEOLOGY*, v. 98, p. 797–818.
- Hitzman, M.W., Reynolds, N.A., Sangster, D.F., Allen, C.R., and Carman, C., 2003, Classification, genesis, and exploration guides for nonsulfide zinc deposits, *ECONOMIC GEOLOGY*, v. 98, p. 685–714.
- Ingwersen, G., 1990, Die sekundären Mineralbildungen der Pb-Zn-Cu-Lagerstätte Tsumeb, Namibia (Physikalisch-chemische Modelle): Unpublished PhD dissertation, Universität Stuttgart, 234 p.
- Large, D., 2001, The geology of non-sulphide zinc deposits, an overview: *Erzmetall*, v. 54, p. 264–276.
- Lohmann, K.C., 1988, Geochemical patterns of meteoric diagenetic systems and their application to studies of paleokarst, in James, N.P., and Choquette, P.W., eds., *Paleokarst: Heidelberg, Springer Verlag*, p. 58–80.
- Mann, A.W., and Deutscher, R.L., 1980, Solution geochemistry of lead and zinc in water containing carbonate, sulphate and chloride ions: *Chemical Geology*, v. 29, p. 293–311.
- Marcello, A., Salvadori, I., and Zuffardi, P., 1965, Prime notizie su un sondaggio eseguito nella valle di Iglesias: *Resoconti Associazione Mineraria Sarda*, v. XX, p. 1–13.
- McCrea, J.M., 1950, On the isotope chemistry of carbonates and a paleotemperature scale: *Journal of Chemical Physics*, v. 18, p. 849–857.
- McDonald, W.S., and Cruickshank, D.W.J., 1967, Refinement of the structure of hemimorphite: *Zeitschrift Kristallographie*, v. 124, p. 180–191.
- Melchiorre, E.B., and Williams, P.A., 2001, Stable isotope characterization of the thermal profile and subsurface biological activity during oxidation of the Great Australia deposit, Cloncurry, Queensland, Australia: *ECONOMIC GEOLOGY*, v. 96, p. 1685–1693.
- Melchiorre, E.B., Criss, R.E., and Rose, T.P., 1999, Oxygen and carbon isotope study of natural and synthetic malachite: *ECONOMIC GEOLOGY*, v. 94, p. 245–260.
- 2000, Oxygen and carbon isotope study of natural and synthetic azurite: *ECONOMIC GEOLOGY*, v. 95, p. 621–628.
- Melchiorre, E.B., Williams, P.A., and Bevins, R.E., 2001, A low temperature oxygen isotope thermometer for cerussite, with application at Broken Hill, New South Wales, Australia: *Geochimica et Cosmochimica Acta*, v. 65, p. 2527–2533.
- Monteiro, L.V.S., Bettencourt, J.S., Spiro, B., Graça, R., and de Oliveira, T.L., 1999, The Vazante zinc mine, Minas Gerais, Brazil: Constraints on willemitic mineralization and fluid evolution: *Exploration Mining Geology*, v. 8, p. 21–42.
- Moore, J.McM., 1972, Supergene mineral deposits and physiographic development in southwest Sardinia, Italy: *Transactions Institution Mining and Metallurgy (Section B: Applied Earth Science)*, v. 71, B59–B66.
- Münch, W., and Siebrat, H., 1960, Rapporto sulle ricerche geologico-giacimentologiche nelle miniere del gruppo Ponente ed Agruxiau, v. I: Unpublished internal report, Azienda Minerali Metallici Italiani, 135 p.
- O'Neil, J.R., 1986, Theoretical and experimental aspects of isotopic fractionation, in Valley, J.W., Taylor, H.P. Jr., and O'Neil, J.R., eds., *Stable isotopes in high temperature geological processes: Mineralogical Society of America Reviews in Mineralogy*, v. 16, p. 1–40.
- O'Neil, J.R., Clayton, R.N., and Mayeda, T., 1969, Oxygen isotope fractionation in divalent metal carbonates: *Journal of Chemical Physics*, v. 51, p. 5547–5558.
- Palache, C., Berman, H., and Frondel, C., 1951, *The system of mineralogy*: New York, Wiley, 1124 p.
- Perna, G., Turi, B., and Vesica, P., 1994, Le calcite delle cavità carsiche del Calcare Miliolitico, in Fadda, A., Ottelli, L., and Perna, G., eds., *Il bacino carbonifero del Sulcis: Geologia, idrologia, miniere: Carbosulcis, Cagliari*, p. 110–114.
- Rosenbaum, J., and Sheppard, S.M.F., 1986, An isotope study of siderites, dolomites and ankerites at high temperature: *Geochimica et Cosmochimica Acta*, v. 50, p. 1147–1150.
- Salvadori, I., 1961, Su alcune particolari mineralizzazioni del Sulcis, Sardegna sud-occidentale: *Resoconti Associazione Mineraria Sarda XV*, v. 65, Iglesias, p. 58–71.
- Sangameswar, S.R., and Barnes, H.L., 1983, Supergene processes in zinc-lead-silver sulfides ores in carbonates: *ECONOMIC GEOLOGY*, v. 78, p. 1379–1397.
- Schwarcz, H.P., 1986, Geochronology and isotope geochemistry of speleothem, in Fritz, P., and Fontes, J.Ch., eds., *Handbook of environmental isotope geochemistry, v. 2: The terrestrial environment*: Amsterdam, Elsevier, p. 271–303.
- Sitzia, R., 1965, Osservazioni su alcune ferrosmithsoniti di Montevecchio: *Atti Symposium Problemi Geo-Minerari Sardi, Associazione Mineraria Sarda, Cagliari-Iglesias*, 1965, p. 434–437.
- Stara, P., Rizzo, R., and Tanca, G.A., 1996, Iglesias-Arburese, miniere e minerali: *Ente Minerario Sardo*, v. I, 238 p.
- Swart, P.K., Burns, S.J., and Leder, J.J., 1991, Fractionation of the stable isotopes of oxygen and carbon during reaction of calcite with phosphoric acid as a function of temperature and method: *Chemical Geology*, v. 86, p. 89–96.
- Takahashi, T., 1960, Supergene alteration of zinc and lead deposits in limestone: *ECONOMIC GEOLOGY*, v. 55, p. 1083–1115.
- Williams, P.A., 1990, *Oxide zone geochemistry*: London, Ellis Horwood Ltd., 286 p.
- Zheng, Y.F., 1999, Oxygen isotope fractionation in carbonate and sulfate minerals: *Geochemical Journal*, v. 33, p. 109–126.
- Zuffardi, P., 1952, Il giacimento piombo-zincifero di Monte Agruxiau: *Industria Mineraria*, v. 3, p. 1–12.